REPORT DOCUMENTATION PAGE

Form Approved
OMB No. 0704-0188

PLEASE DO NOT RETURN YOUR FORM TO THE ABOVE ORGANIZATION.

1. REPORT DATE *(DD-MM-YYYY)*	2. REPORT TYPE	3. DATES COVERED *(From - To)*
30/11/2011	Quarterly	01/09/2011 to 30/11/2011

4. TITLE AND SUBTITLE
Thin Film Photovoltaic Cells on Flexible Substrates Integrated with Encrgy Storage

5a. CONTRACT NUMBER

5b. GRANT NUMBER
N00014-11-1-0658

5c. PROGRAM ELEMENT NUMBER

6. AUTHOR(S)
Westgate, Charles R. Sr.
Director of the Center for Autonomous Solar Power

5d. PROJECT NUMBER

5e. TASK NUMBER

5f. WORK UNIT NUMBER

7. PERFORMING ORGANIZATION NAME(S) AND ADDRESS(ES)
Center for Autonomous Solar Power
Binghamton University
85 Murray Hill Road
Vestal, NY 13850

8. PERFORMING ORGANIZATION REPORT NUMBER
Q-Nov-2011

9. SPONSORING/MONITORING AGENCY NAME(S) AND ADDRESS(ES)
Office of Naval Research
875 North Randolf Street
Arlingtonm VA 22203-1995

10. SPONSOR/MONITOR'S ACRONYM(S)
ONR

11. SPONSOR/MONITOR'S REPORT NUMBER(S)

12. DISTRIBUTION/AVAILABILITY STATEMENT
Unlimited, public

13. SUPPLEMENTARY NOTES

20111214044

14. ABSTRACT

The goals of the research program in the Center for Autonomous Solar power are to conduct research and development in thin film solar cells on flexible substrates for low cost fabrication on roll-to-roll manufacturing. The materials chosen for the cells are earth abundant and non-toxic. The expected outcome is very low cost solar cells that will be competitive in performance and well below current market prices in dollars/watt. Flexible solar cells are useful in building integrated photovoltaic voltaic systems and in military applications in austere environments.

A related research program focuses on ultracapacitors using new materials as well. With sufficiently high energy densities, ultracapacitors can replace batteries for energy storage and offer other advantages in lifetime and in tolerating a wider operating temperature range.

15. SUBJECT TERMS
Solar cells, thin films

16. SECURITY CLASSIFICATION OF:			17. LIMITATION OF ABSTRACT	18. NUMBER OF PAGES	19a. NAME OF RESPONSIBLE PERSON
a. REPORT	b. ABSTRACT	c. THIS PAGE			Charles R. Westgate
U	U	U	UU	38	19b. TELEPHONE NUMBER *(Include area code)* 607-777-6598

Thin Film Photovoltaic Cells on Flexible Substrates Integrated with Energy Storage

Award Number N00014-11-1-0658

PI: Charles R. Westgate
Binghamton University
Binghamton, NY 13902
607-777-6598
607-777-5780 (fax)
westgate@binghamton.edu

Project Period:	June 1, 2011 through August 31
Reporting Period:	September 11, 2011 to November 30, 2011
Date:	November 30, 2011

Project Overview

The goals of the research program in the Center for Autonomous Solar power are to conduct research and development in thin film solar cells on flexible substrates for low cost fabrication on roll-to-roll manufacturing. The materials chosen for the cells are earth abundant and non-toxic. The expected outcome is very low cost solar cells that will be competitive in performance and well below current market prices in dollars/watt. Flexible solar cells are useful in building integrated photovoltaic voltaic systems and in military applications in austere environments.

A related research program focuses on ultracapacitors using new materials as well. With sufficiently high energy densities, ultracapacitors can replace batteries for energy storage and offer other advantages in lifetime and in tolerating a wider operating temperature range.

Solar cells consist of three critical layers: a transparent conductor, an n-type layer that is also transparent, and a p-type material that is strongly absorbing. The Center's research on thin film materials includes replacing the conventional indium tin oxide (ITO) used as a transparent conductor with aluminum doped zinc oxide. Indium is a rare and expensive material, and ITO is brittle, making it less suitable for flexible substrates.

For the n-type material, we have successfully achieved high quality films using zinc sulfide. This layer replaces cadmium sulfide which is much less desirable because of toxicity. The p-type substrates candidates include iron disulfide, zinc phosphide, and copper zinc tin sulfide CZTS). These materials have near optimum bandgaps, absorb strongly, and have high mobilities (or equivalently, high diffusion constants). We have successfully deposited high quality films of all critical cell lays, including the three candidate p-type layers.

Of the three p-type candidates, CZTS is the most promising. Optimization of the deposition processes has begun. At Binghamton, pulsed laser deposition and chemical vapor deposition

have been studied. A subcontract to Clarkson University has begun to deposit this material using a chemical process. These are all alternatives to processes currently used elsewhere (e.g., IBM) that use a highly toxic and unstable gas considered unsafe in academic settings.

Solar cells have been fabricated in the CASP laboratories but have not yet yielded high efficiencies. Studies are underway to determine the sources of losses and to modify the layers or deposition processes appropriately.

On ultracapacitors, research has begun on electrodes and electrolytes to improve energy densities. Additional details follow in this report. A subcontract to the Naval Research Laboratory has begun as part of this effort.

In addition to formation of layers and cells, reliability studies have been conducted on some flexible substrates and layers. Recent results are included below. The Center is a founding member of a consortium of universities and companies in testing solar cells. Funding for this program is provided by the New York State Energy Research and Development Agency (NYSERDA). The Center is also a grantee on an education program in solar cells. A small study on a novel technique for non-contact measurements of Hall mobility is also underway and shows very promising results. Funding to support this measurement effort will be sought from another agency. Some of these efforts will be described below.

TASK Report

The major research projects in the center include:

- Transparent conductors for solar cells
- Thin film solar cells using earth abundant materials with three candidate p-type absorbers
- Ultracapacitors for solar energy systems
- Reliability and durability of thin film solar devices
- Thermoelectric solar devices
- Hybrid organic/inorganic solar cells

A kickoff meeting with a team from ONR, NRL, and ARL was held on November 17, 2011 during which presentations were made on most of the tasks. The team also received a written report before they arrived, and those materials will not be repeated here.

A summary of activities including new reports follow.

1. Transparent conductors for solar cells Tara Dhakal

The initial aluminum doped zinc oxide (AZO) films were deposited used an atomic layer deposition (ALD) instrument that produced very high quality films. The ALD was on loan and was recalled to its home institution. We are purchasing a replacement. The ALD produces conformal layers that help minimize pinholes or other defects that can promote leakage. We

have been successful in producing good quality films with sputtering. The roll-to-roll line at Binghamton University will be ready to test deposition of AZO in early 2012 on a variety of flexible substrates. One of the more promising substrates is a 75 micron thick flexible glass manufactured by Corning. Corning has recently produced rolls of the glass and tested it on the Binghamton roll-to-roll line. Glass offers several advantages to solar cells including the ability to tolerate higher temperatures and serve as more effective barrier to moisture that can damage any solar cell. During the next quarter, we will prepare samples of AZO on flexible substrates in the roll-to-roll facility and evaluate the promise of larger scale production and reliability. The durability of the glass to cracks is, of course, and important issue that we will investigate.

A 1000 hour test on a variety of AZO coated substrates was recently concluded. The test cycled temperatures and humidity hourly between low temperatures and low humidity to higher levels: 80^0 C and 80% humidity. The samples included films deposited by a commercial firm and sputtered films deposited by CASP. This thinnest samples (less than 200 nm) exhibited apparent damage. The thicker films did not exhibit obvious damage; however additional characterization of the films will be done.

2. **P-type absorbers** – Parag Vaseker, Lakshmi Ganta, and Siva Adusumilli, Binghamton. Professor Ian Suni, Clarkson.

Results of research on two of the three p-type absorbers are reported here. The third candidate, iron disulfide will be discussed in the next report. The report by Professor Suni is attached at the end of the quarterly report.

A. Synthesis of Zn_3P_2 thin films

Zn_3P_2 has already been optimized in both nanowire and thin film form. It was observed in the above set-up that when the evaporated zinc on the substrate is facing up, it is exposed to TOP vapors and during this condition, nanowires of zinc phosphide are formed. On the other hand, when the evaporated zinc is facing down and exposed to liquid TOP, a thin film of zinc phosphide is synthesized. SEM images of the zinc phosphide thin film are as shown in Fig.1

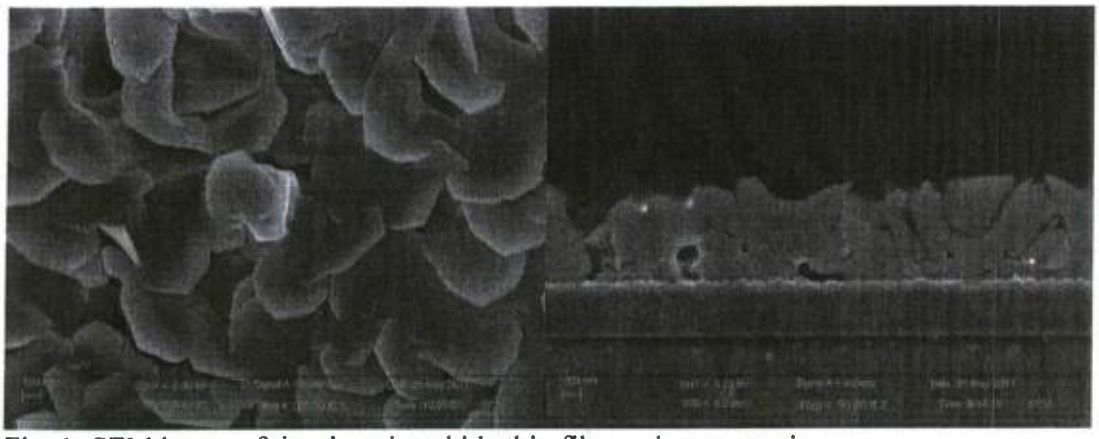

Fig. 1: SEM image of the zinc phosphide thin film and cross-section.

As seen in Fig.2, well-faceted grains of zinc phosphide are synthesized with average diameter ~ 400-500 nm. In the cross-section, the thickness of half a micron of zinc phosphide can be seen on the Molybdenum-coated glass structure. The elemental analysis from EDAX gives Zn- 59% and P-41% which is very close to stoichiometric composition of tetragonal Zn_3P_2 structure.

Fig.2 shows XRD data for the zinc phosphide film. The peaks closely match JCPDS- 22-1021 for tetragonal zinc phosphide phase.

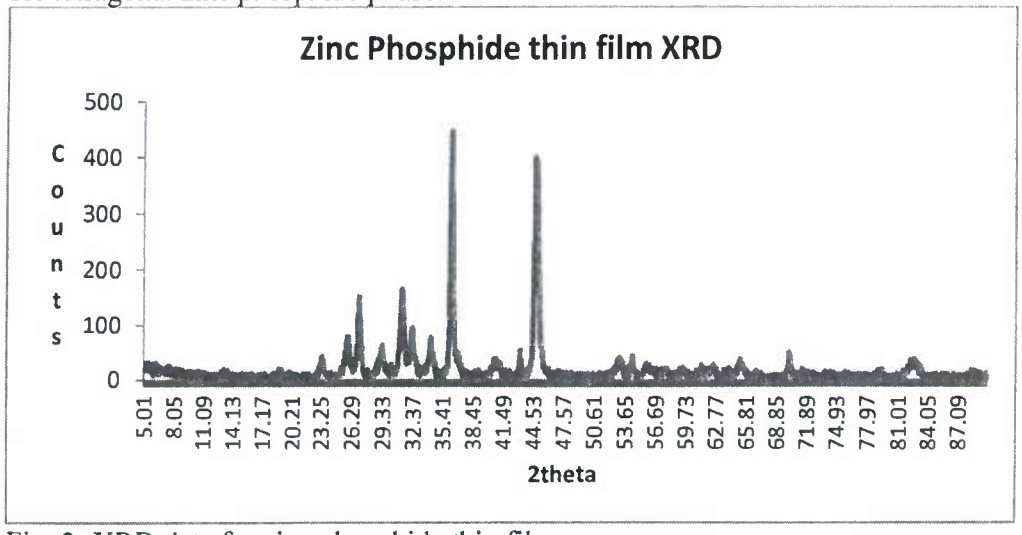

Fig. 2: XRD data for zinc phosphide thin film.

Figure 3 shows XPS binding energy peaks at 1020.6 eV for Zn $2p_{3/2}$,139 eV for Zn 3s and 127.80 eV for P $2p_{3/2}$. XPS analysis confirms Zn_3P_2 phase and atomic concentrations determined by XPS are 61% zinc and 39% phosphorous.

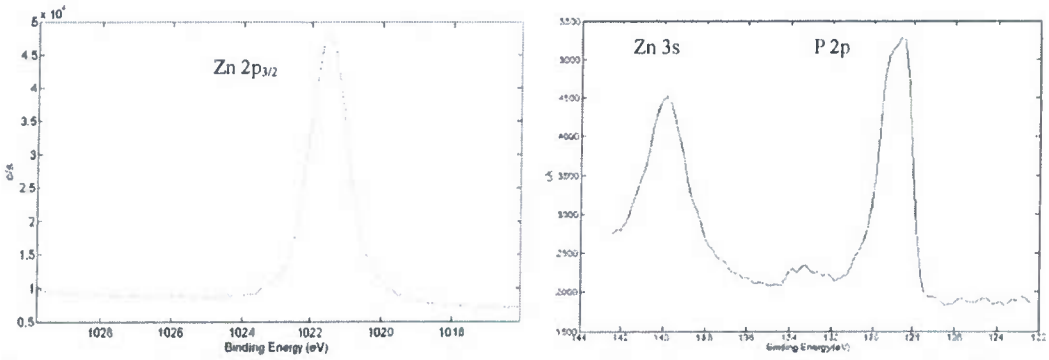

Figure 3: XPS binding energy peaks for zinc and phosphorous in the Zn_3P_2 thin film

Plans for coming quarter:

En route to completion of zinc phosphide hetero-junction cells, experiments have been conducted to cross-check the chemical compatibility of n-type partners CdS and ZnS with zinc phosphide films and hetero-junctions of both types have been successfully completed. Zinc phosphide solar cells are being completed with n-type hetero-junction partners ZnS and ZnO and initial results show diode behavior. Photovoltaic parameters are being analyzed to determine the cause for the losses. One important reason is that ZnO and AZO layers are in a development phase by sputtering. Once these layers are optimized, there can be reasonable improvement in the photovoltaic parameters. Also all the cells will be analyzed using photoluminescence and quantum efficiency measurements. Electrical and 0ptical characterization will also be carried out on the zinc phosphide films.

B. Synthesis of CZTS thin films using TBDS as a sulfur source

Thin film solar cells based on $Cu(In,Ga)(S,Se)_2$ and CdTe have demonstrated significant improvement in last few years and they are being transferred to production levels [1,2]. Of these two technologies, CIGS based solar cells are the most efficient ones at the laboratory level and have demonstrated efficincies in the range of ~20% [3]. However, both CIGS and CdTe based thin film solar cells are hindered by potential environmental hazard issues[4] and scarcity issues associated with the constituent elements , mainly Te, In, Ga and to some extent Se[4,5]. Recent research trends are moving towards finding alternatives based on earth-abundant and non-toxic elements. An alternative material $Cu(Zn,Sn)(S,Se)_2$ is under study by the thin film photovoltaics community which contains earth abundant materials like Zn and Sn. CZTS structures can be derived from $CuInS_2$ chalcopyrite structure by replacing one half of the constituent indium atoms by zinc and other half by tin. The resulting bandgap varies in the range of 0.8 eV for a selenide structure to 1.5 eV for a sulfide structure[6]. Copper and sulfur in earth's crust are 50 and 260 ppm respectively and while abundance of zinc and tin is 75 and 2.2 ppm in respectively. As compared to this, indium in earth's crust is 0.049 ppm and selenium 0.05 ppm. Several preparation methods have been reported in literature for preparation of CZTS solar cells . These are Physical vapor methods (sulfurization of e-beam evaporated metallic layers and sputtered layers [7,8], RF magnetron sputtering[9], co-evaporation[10], hybrid sputtering[11]). Chemical methods involve sulfurization of electrochemically deposited metalllic precursors[12], photochemical deposition[13], sol-gel sulfurization methods[14], sol-gel spin-coated deposition[15] and spray pyrolysis[16,17][16-18]. In addition, there is synthesis based on solution methods[18]. In 1988, Nakazawa et al reported the photovoltaic effect in a heterodiode of CZTS for the first time and open-circuit voltage of 165 mV[19]. In 2008, Katagiri et al

obtained an efficiency of 6.7% by Physical vapor methods[20]. In 2010, Mitzi et al reported an efficiency of 9.6% by solution methods[21] . CZTS also has a large absorption coefficient in the order of 10^4 cm^{-1}[20].

Results

The process used for sulfurization is same as described above in the zinc sulfide section. SEM images of samples sulfurized at different temperatures are as follows:

Sample 1: 300°C, 60 min

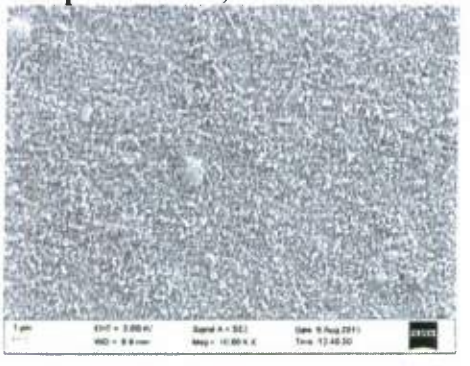

EDAX atomic percentages: Cu-28.2%,Zn-15.8%,Sn-17.6% and S-38.4%

Sample 2: 350°C, 60 min

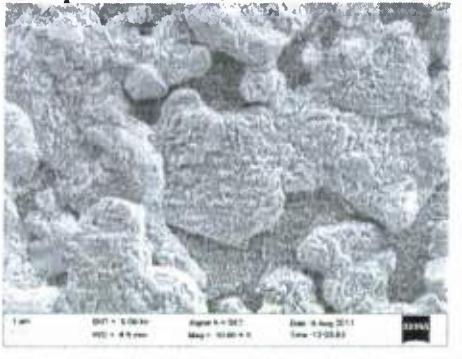

EDAX atomic percentages: Cu-43.85%,Zn-11.18%,Sn-14.31% and S-30.66%

Sample 3: 400°C, 60 min

EDAX atomic percentages: Cu-18.62%,Zn-12.9%,Sn-24.99% and S-44.31%

Sample 4: 500°C, 60 min

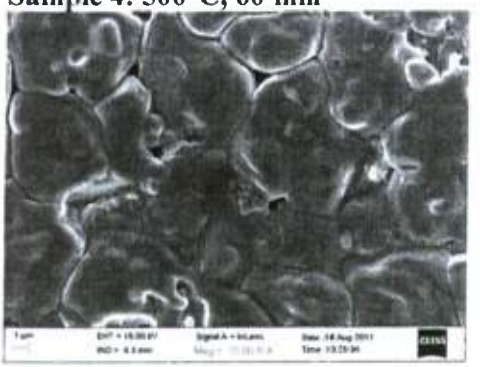

EDAX atomic percentages: Cu-24.59%,Zn-12.99%,Sn-13.12% and S-49.31%

It can be observed that CZTS thin films with stoichiometric composition and well-defined grains with diameter around 2 microns are obtained at 500°C and 60 min

XRD Results

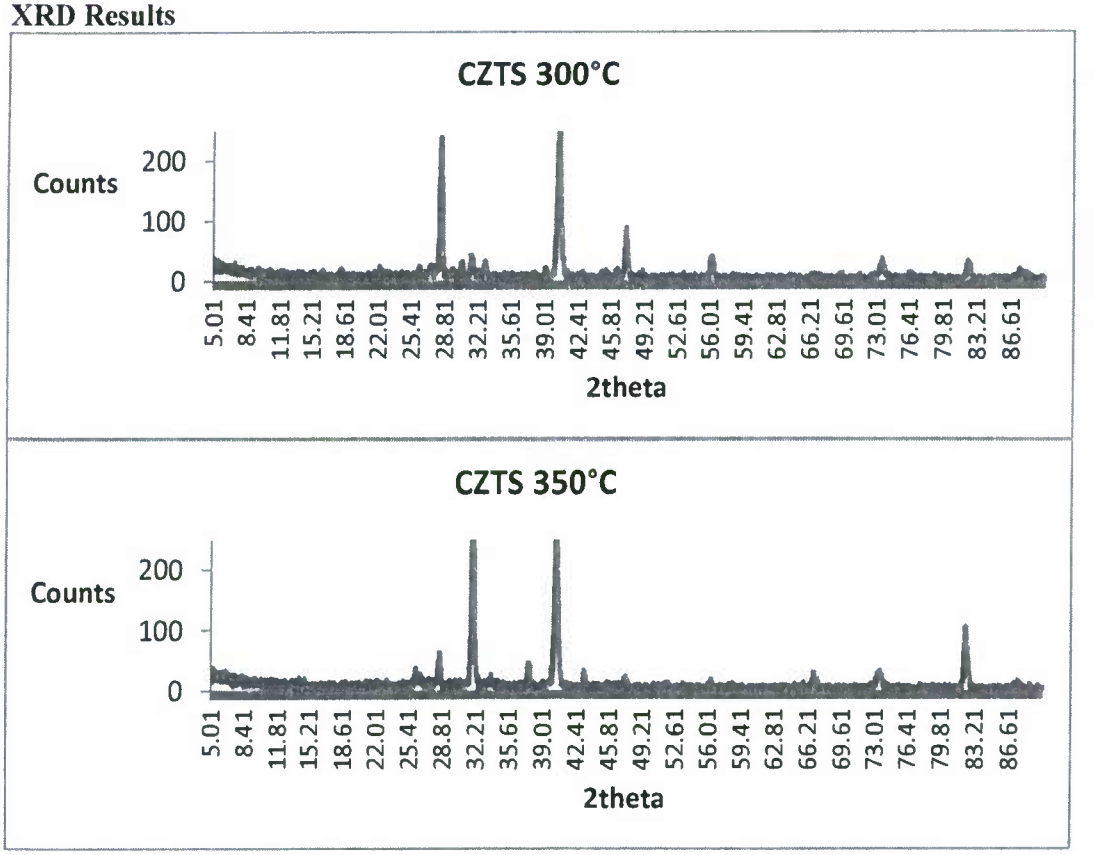

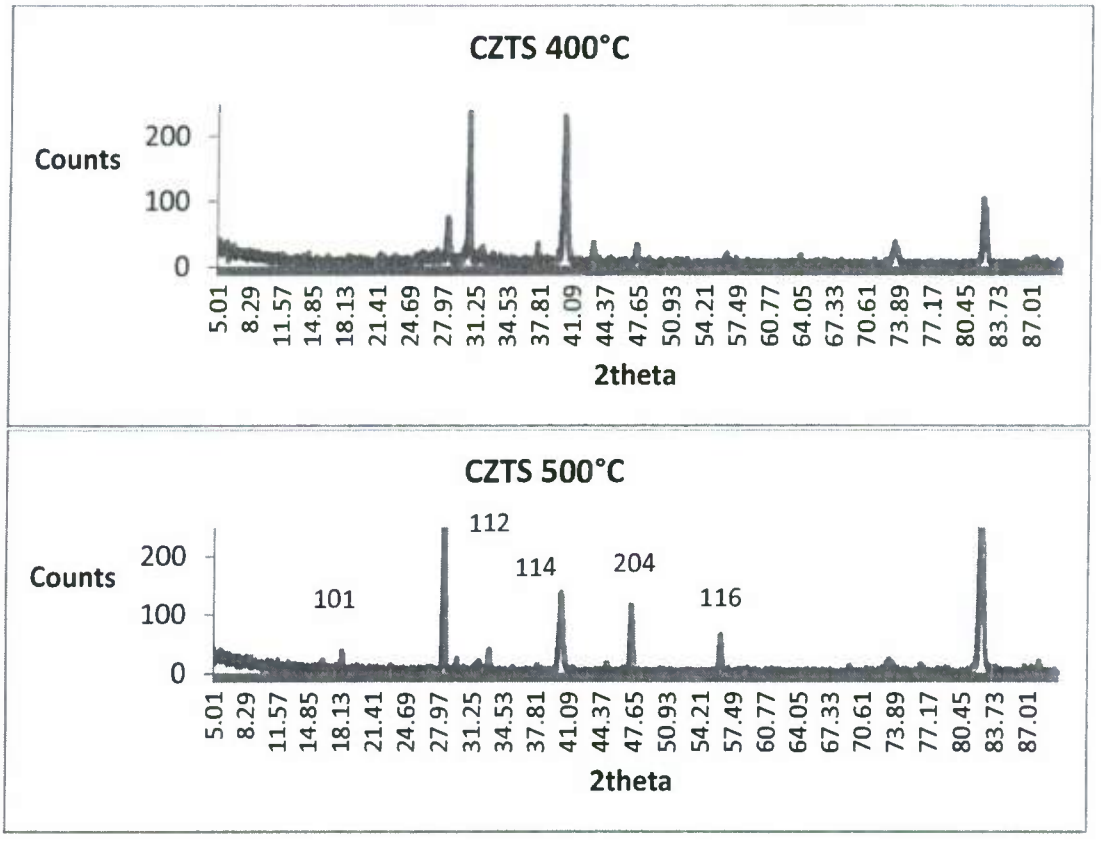

It can be seen that 112-oriented Kesterite phase is confirmed at 500°C according to PDF 00-021-088.

AFM Results

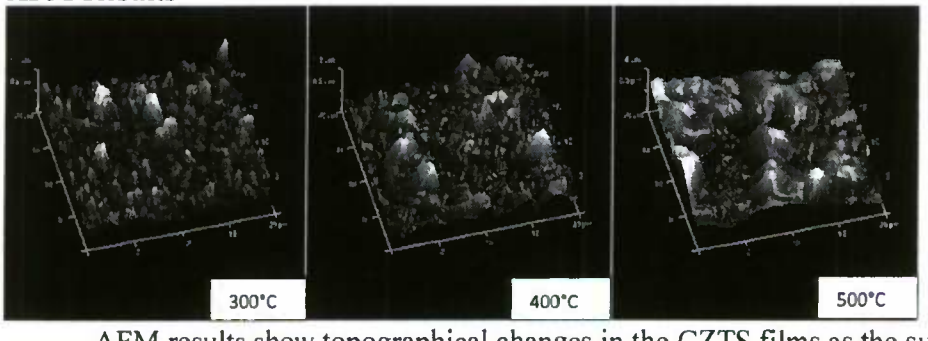

AFM results show topographical changes in the CZTS films as the sulfurization temperature is increased from 300°C to 500°C. It can be observed that at 500°C, the grain size is large, compact and the film is smoother.

Plans for coming quarter:

CZTS films have been successfully synthesized using TBDS in the CVD set-up. The films have been optimized and confirmed using various analytical techniques. Initial test cells have been prepared and they exhibit diode behavior confirming the p-n junction. Both CdS and ZnS have been used as n-type hetero-junction partners. Near term plans include determining the exact phase of CZTS and avoiding secondary phases. Raman spectroscopy will be used for this

purpose if possible. Also the completed cells will be analyzed using photoluminescence and quantum efficiency measurements. Electrical and optical characterization will also be carried out on these films.

References

[1] N.G. Dhere, Solar Energy Mater. Solar Cells 91 (2007) 1376.
[2] N.G. Dhere, Solar Energy Mater. Solar Cells 95 (2011) 277.
[3] I. Repins, M. Contreras, M. Romero, Y. Yan, W. Metzger, J. Li, S. Johnston, B. Egaas, C. DeHart, J. Scharf, B.E. McCandless, R. Noufi, In: Anonymous Photovoltaic Specialists Conference, 2008. PVSC '08. 33rd IEEE, (2008) 1.
[4] M.M.A. Green, Progress in photovoltaics 14 (2006) 383.
[5] B.B.A. Andersson, Progress in photovoltaics 8 (2000) 61.
[6] H. Katagiri, Thin Solid Films 480 (2005) 426.
[7] H. Araki, Thin Solid Films 517 (2008) 1457.
[8] H. Katagiri, N. Sasaguchi, S. Hando, S. Hoshino, J. Ohashi, T. Yokota, Solar Energy Mater. Solar Cells 49 (1997) 407.
[9] J. Seol, S. Lee, J. Lee, H. Nam, K. Kim, Solar Energy Mater. Solar Cells 75 (2003) 155.
[10] T. Tanaka, D. Kawasaki, M. Nishio, Q. Guo, H. Ogawa, physica status solidi (c) 3 (2006) 2844.
[11] T. Tanaka, T. Nagatomo, D. Kawasaki, M. Nishio, Q. Guo, A. Wakahara, A. Yoshida, H. Ogawa, Journal of Physics and Chemistry of Solids 66 (2005) 1978.
[12] H. Araki, Y. Kubo, A. Mikaduki, K. Jimbo, W.S. Maw, H. Katagiri, M. Yamazaki, K. Oishi, A. Takeuchi, Solar Energy Mater. Solar Cells 93 (2009) 996.
[13] K. Moriya, J. Watabe, K. Tanaka, H. Uchiki, physica status solidi (c) 3 (2006) 2848.
[14] K. Tanaka, M. Oonuki, N. Moritake, H. Uchiki, Solar Energy Mater. Solar Cells 93 (2009) 583.
[15] M.M.Y. Yeh, J. Sol Gel Sci. Technol. 52 (2009) 65.
[16] N. Nakayama, K. Ito, Appl. Surf. Sci. 92 (1996) 171.
[17] N. Kamoun, H. Bouzouita, B. Rezig, Thin Solid Films 515 (2007) 5949.
[18] S.C. Riha, B.A. Parkinson, A.L. Prieto, J. Am. Chem. Soc. 131 (2009) 12054.
[19] T.N. K.Ito , Japanese journal of Applied Physics (1988).
[20] H. Katagiri, K. Jimbo, W.S. Maw, K. Oishi, M. Yamazaki, H. Araki, A. Takeuchi, Thin Solid Films 517 (2009) 2455.
[21] T.K. Todorov, K.B. Reuter, D.B. Mitzi, Adv Mater 22 (2010) E156.

3. **Energy Storage: Ultracapacitors** - Professor Rastogi and Gaind Pandey

During the kickoff presentations, reports were made on the progress on ultracapacitors including the subcontract work at NRL. The NRL work was presented by Dr. Megan Sassin on behalf of Dr. Jeffrey Long who could not be present. Following is a brief update.

This report embodies the research and development work carried out and the progress achieved in the three major areas of the program of solid state supercapacitors for solar electricity storage. The areas and the major tasks therein are: (i) Supercapacitor Electrodes: based on the

conducting polymers and its nanocomposite utilizing the electro-active metal oxides to take advantage of multiple charge storage regimes and achieve both high energy density storage and stable performance under repeated charge-discharge cycles, (ii) Solid Electrolytes: based on both organic and inorganic ions in the form of gels which display high electrical conductivity, high voltage break-down range and increased charge transfer performance and (iii) Solid-State Supercapacitors: based on novel substrates and by utilizing inexpensive electrode preparation methodologies, work on supercapacitor fabrication and performance evaluations.

Progress Report:

Electo-active Supercapacitor Electrodes Synthesis

MnO_2 enriched nanostructured conducting polymer on carbon paper for supercapacitor

A major emphasis is on developing conducting polymer nanocomposite electrodes for supercapacitors. Currently, the research work is conducted on various π-conjugated theophene based conducting polymers (T-CP) and their nanocomposites with the pseudo-capacitive metal-oxides. Research is being done on various electrochemical and chemical routes for synthesis of these materials. From our work, the most useful synthesis route is based on the electro-polymerization from monomer species. For the fabrication of metal oxide nanocomposites, polymer synthesis *insitu* with metal-oxide as well as impregnation of metal oxide post polymer synthesis are being developed. Conducting polymer synthesis is carried out by galvanic pulse polymerization technique over various carbon based substrates. Typically, the galvanic pulse polymerization was carried out using the monomer with suitable anion species such as ClO_4, SO_4 etc. in an organic medium such as acetonitrile and similar solvents. The molar concentration of the monomer and anion species was optimized, typically at 0.01M and 0.1M, respectively. The synthesis was done in electrochemical cell with a platinum counter electrode using galvanic pulses as described in the previous report.

For the nanocomposite synthesis, MnO_2 nanoparticles were loaded within the pores of the conducting polymer film. This was achieved by soaking the as-electrochemically deposited polymer film in a potassium permanganate solution of different concentrations (10-50 mM). The solution molarities were optimized depending on the desired amount of MnO_2 nanoparticles to be embedded [1]. Since, the permanganate solution under acidic environment is a strong oxidizing reagent, it is important not to over-oxidize the conducting polymer. This is achieved by use of neutral permanganate solution with low (typically 10 mM) concentration and by using short (typically 10 min) treating time.

Gel polymer electrolyte Investigations

In the search for solid-state forms of electrolytes for supercapacitors we have experimented with several ionic liquids immobilized in various polymer matrices. Our research led to standardized electrolyte which uses BMIM-BF_4 and EMIM-BF_4 ionic liquids in PVdF-HFP polymer matrix. A practical gel-like form for use with solid-state supercapacitors was developed by a solution cast method. For enhanced performance, a 4:1 ratio of ionic liquid to polymer was standardized. The

ratio of host polymer to active ionic component is critical to achieve improved supercapacitor energy density values and stability.

Cell fabrication and characterization techniques

For the supercapacitor fabrication electroactive polymer layers were coated on flexible graphite sheets and carbon paper by the electrochemical polymerization technique as described above. All-solid-state supercapacitor cells were fabricated using well characterized and identically performing symmetrical polymer electrodes. These electrodes were interspaced to an optimal thickness and with agel polymer electrolyte layer sandwiched in between. Various methods including the solvent evaporation were applied to incorporate electrolyte. Supercapacitor fabrication was completed with application of the contact tabs. Fig. 1 shows a typical supercapacitor cell made on a carbon paper.

The supercapacitor cells were characterized for the capacitance density and charge-discharge performance. To provide scientific data on the mechanism and stability of supercapacitors, both ac impedance spectroscopy in the frequency range from 10 mHz to 100 kHz and cyclic voltammetry in the scan range 10 -100 mV/s rate was carried out.

Fig. 1: Digital image of a supercapacitor cell

Characterization of Nanocomposite Polymeric Electrodes:

Considering that the polymer morphology is critical to the achievement of high energy density, we carried out extensive optimizing studies of the morphology during stages and parameters used for the growth of polymer and nanocomposite films and the effects of the substrate surface. A FESEM image in Fig. 2 shows typical result of the surface morphology of a theophene based conducting polymers (T-CP) treated with the permanganate solution for embedding MnO_2 nanoparticles. A high resolution SEM image of the nanocomposite film on a carbon paper confirms finely dispersed MnO_2 nanoparticles within the pore and surface of the polymer. Further, the EDAX data shown in Fig. 2(c) also confirm the reduction of $KMnO_4$ into MnO_2. In order to sustain and achieve pseudo-capacitive properties of the MnO_2 nanoparticles, valence state of the Mn is an important issue. We carried out extensive analysis of the films using the x-ray photo-electron spectroscopy (XPS) technique. Figure 3 shows the XPS spectra obtained from a (T-CP) polymer film with embedded MnO_2 nanoparticles. The peaks of Mn $2p_{3/2}$ and Mn $2p_{1/2}$, which are centered at 643 and 653.8 eV, respectively, with a spin energy separation of 11.8 eV,

are in good agreement with reported data of Mn $2p_{3/2}$ and Mn $2p_{1/2}$ in MnO_2 confirming the nanoparticle species are basically highly electro-active MnO_2 species in the films we have formed [2].

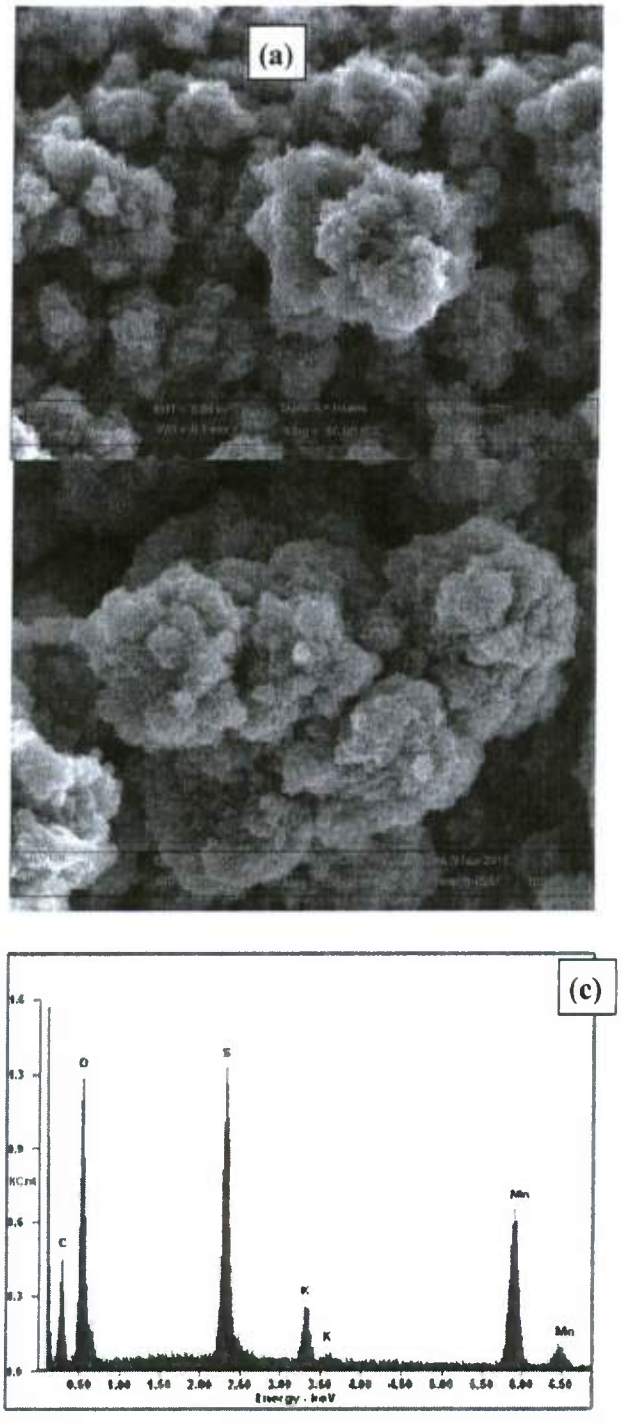

Fig. 2: (a) FESEM image of (a) PEDOT matrix on carbon paper, (b) MnO_2 embedded PEDOT matrix on carbon paper and (c) EDAX spectra of PEDOT-MnO_2 composite electrode.

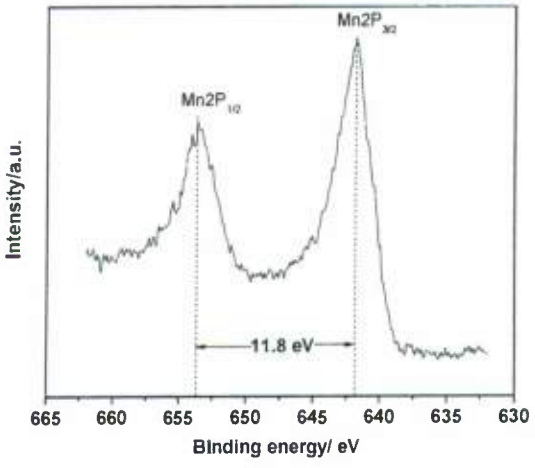

Fig. 3: XPS spectra for manganese in the $KMnO_4$ treated conducting polymer film

Supercapacitor Performance Data

The capacitive performance of the supercapacitors based on the conducting polymer nanocomposite electrodes was evaluated by cyclic voltammetry (CV) and galvanic charge-discharge studies in the two-electrode system using BMIM-BF_4 ionic liquid based gel polymer electrolyte which performs both as an electrolyte as well as separator

Cyclic voltammetry:

Typical CV plots of the supercapacitor cell are shown in Fig. 4 (A) at different scan rates between the floating potentials with the range -1V to +1V. The voltammograms are featureless without any peaked structure at lower (5-20 mV s^{-1}) scan rates. These show almost a square shape, which signifies the basic characteristic of a good supercapacitor.

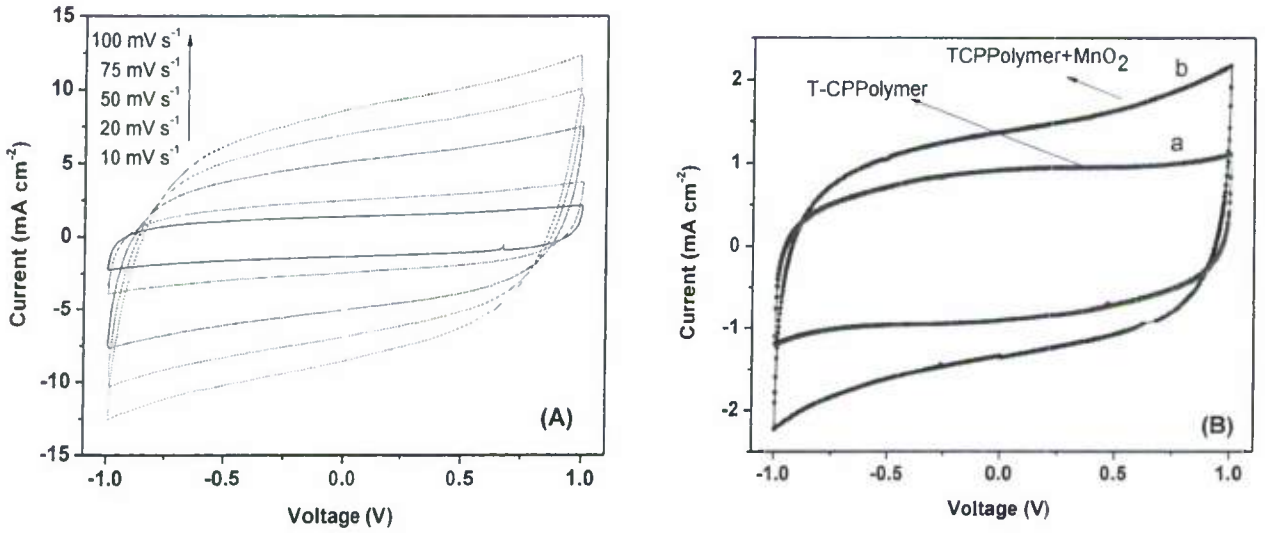

Fig.4: (A) Cyclic voltammograms of the supercapacitor cell with conducting polymer-MnO_2 composite electrode at different scan rates. (B) Typical Cyclic voltammograms of conducting polymer electrode (a) and conducting polymer-MnO_2 composite electrode (b) at 10 mV s^{-1} scan rate.

An insignificant deviation/tilt from the squared shape of the C-V curves at a higher scan rate is caused by small values of the equivalent series resistance (ESR), which is present in all capacitors. Further, the response of each capacitor cell has been found to be scan rate dependent. To establish the efficacy of the nanocomposite electrodes developed in this work, a comparison of the supercapacitor cell performances using the T-CP polymer and the T-CP+MnO_2 nanocomposite electrodes were made. Both cells were fabricated and characterized with the same gel polymer electrolyte. Fig. 4B shows the C-V performance scanned at 10 mV s^{-1} for both these cells. An enhanced electrochemical activity is clearly observed due to the embedding of the MnO_2 within the polymer matrix. However, as the comparison of the CV curves in Fig. 4B reveal, the value of ESR is slightly increased due to MnO_2.

Charge-Discharge Characteristics:

Galvanic charge-discharge experiments were performed for both the supercapacitor cells. Fig. 5A shows the typical charge-discharge plots of supercapacitor cell with nanocomposite electrode at different constant current. Fig. 5B shows a comparative charge-discharge curve at 1 mA cm^{-2} of cells with both the electrode. These cells were charged up to 1.2 V within the maximum stable potential for the conducing polymer electrodes. Confirmation of the capacitive behavior of both

the supercapacitor cells was obtained from the linear discharge characteristics. A sudden drop while discharging at constant current density indicative of the ohmic loss due to ESR is minimal in most of the tested supercapacitors. The capacitance value is increased significantly due to the presence of MnO_2 in the polymer matrix.

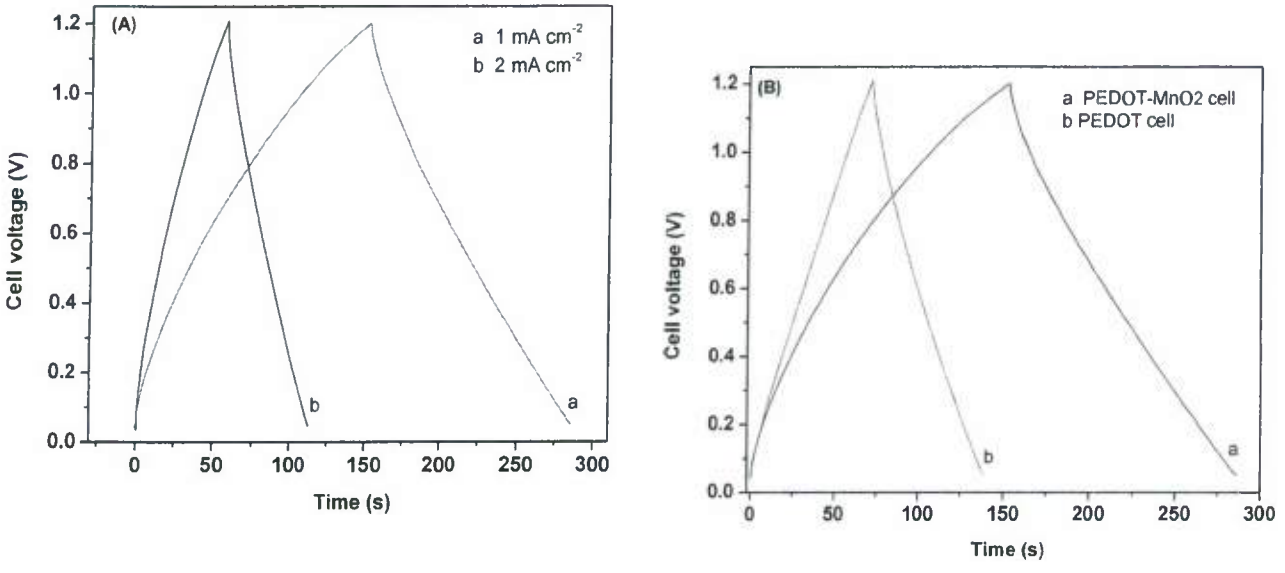

Fig. 5: Charge-discharge curves of supercapacitor cell with conducting polymer-MnO_2 composite electrode (A), and comparative charge-discharge plot with both the electrode at 1mA cm^{-1} (B).

Charge Discharge Stability:

We carried out extensive stability tests on the supercapacitors by sequentially subjecting them to repeated charge-discharge (C-D) cycles. Fig. 6 shows the typical charge-discharge curves observed after increasing numbers of the sequential numbers of C-D cycles as indicated in the figure. The supercapacitor cell under C-D cycle test was fabricate with the nanocomposite electrodes. Cycling tests were performed in the 1V and 0.1 V voltage range at a constant current density of 1 mA cm^{-2}. The capacitance value of the cell in the each cycle number was subsequently calculated from the discharge profiles.

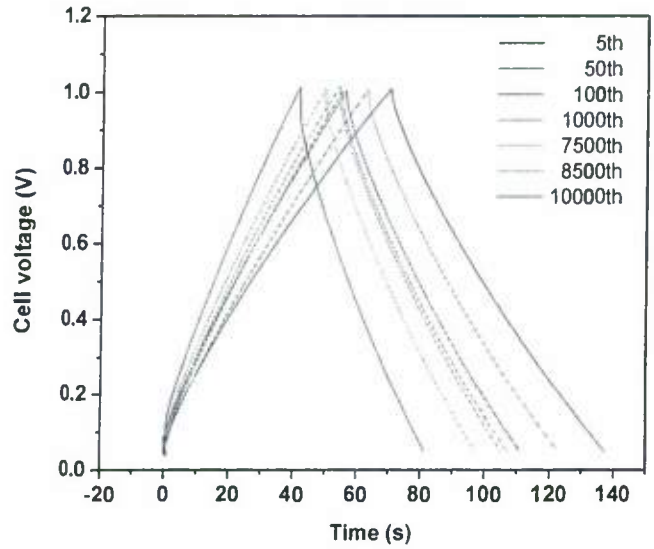

Fig. 6. Typical charge-discharge curve obtained after an increasing numbers of C-D cycle tests.

Fig 7 shows the variation in discharge capacitance (C_d) as a function of the charge-discharge cycle numbers. An initial decrease for the first few C-D cycles, the values of C_d have been observed to be stable for nearly 8000 cycles. A gradual fading is observed beyond 8000 C-D cycels till 10000 cycles.

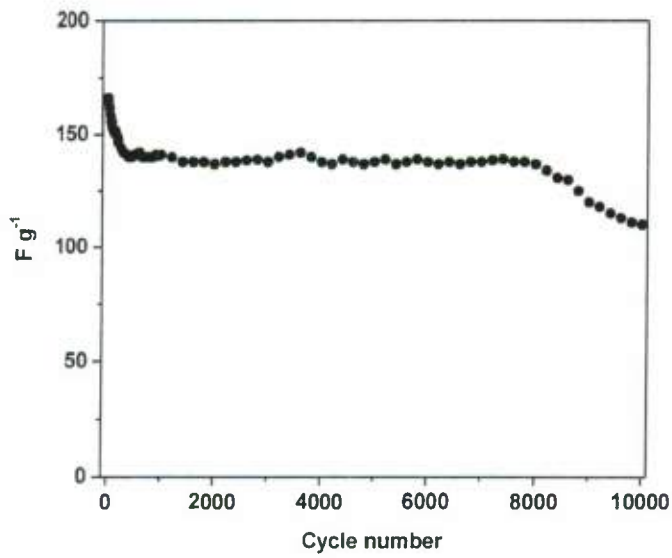

Fig.7. Variation in the discharge capacitance as a function of the charge-discharge cycles at a constant current of 1.0 mA cm^{-2}.

Conclusions:

- The capacitance value obtained from charge-discharge studies of the solid-sate supercapacitors are summarized in table below:

Solid-State Supercapacitor Cells	**With T-CP electrode**	**With T-CP-MnO_2 electrode**
Single electrode capacitance (F g^{-1})	115-120	160-165
Overall cell capacitance (at 1 mA cm^{-1}) (mF cm^{-2})	60-65	95-100

- We achieved high capacitance density values ~160-165 F g^{-1} in solid state form. These values are close to those of liquid electrolytes which are known to give higher performance. This work holds promise for integration with the solar cell modules.

References

[1] R. Liu, J. Duay, S.B. Lee, ACS Nano, 4 (2010) 4299-4307.
[2] A.L.M. Reddy, M.M. Shaijumon, S.R. Gowda, P.M. Ajayan

Summary

Individual layers of solar cells have been fabricated and characterized that indicate good quality films. Solar cells have been fabricated but have demonstrated only low efficiencies. The losses may be due to interface states and other defects in the films, hence extensive electrical and optical studies of the individual layers and cells will be conducted. The results will be used to modify as needed the deposition processes and fabrication to increase efficiencies.

Confidential

Clarkson UNIVERSITY
Ian J. Sunu, Professor
Dept of Chemical and Biomolecular Engineering
Clarkson University
Potsdam, NY 13699-5705
Phone: 315-268-4471
Email: isunu@clarkson.edu

October 31, 2011

To: Roger Westgate, PhD
Center for Autonomous Solar Power (CASP)
Binghamton University
P.O. Box 6000
Binghamton, NY 13902-6000

Re: Progress report, "Electrodeposition of Cu_2ZnSnS_4 (CZTS) with Controlled Stoichiometry"

Executive Summary:

We report the following accomplishment for this project:

- We have begun cyclic voltammetry studies of Cu, Zn, Sn and S in aqueous solutions containing a variety of different complexing agents.

Tasks and Objectives:

Our first objective is to find one or more complexing agents that will shift the equilibrium reduction potentials of Cu and Sn in the cathodic direction. This will allow simultaneous electrodeposition of Cu, Sn and Zn at the same reduction potential. Without complexing agents, the standard reduction potentials of these three elements are:

$$Cu^{2+} + 2e^- \rightarrow Cu \qquad E^0 = +0.340V \text{ vs. } NHE$$
$$Zn^{2+} + 2e^- \rightarrow Zn \qquad E^0 = -0.763V \text{ vs. } NHE$$
$$Sn^{2+} + 2e^- \rightarrow Sn \qquad E^0 = -0.136V \text{ vs. } SHE$$

Without substantially shifting the equilibrium reduction potential for Cu, Cu deposition will be extremely rapid at the highly cathodic potentials at which Zn deposition is possible. In other words, the electrodeposit will contain far more Cu than Zn, so we need to slow Cu electrodeposition through use of a complexing agent. S electrochemistry will also be investigated, but is more complex than that of Cu, Zn and Sn, so the standard reduction potential is not given above.

In addition, we will inspect our cyclic voltammograms for solutions that contain Cu, Zn, Sn and S for evidence of the induced co-deposition mechanism. Evidence for

Confidential

Clarkson UNIVERSITY defy convention

Ian I. Suni, Professor
Dept of Chemical and Biomolecular Engineering
Clarkson University
Potsdam, NY 13699-5705
Phone: 315-268-4471
Email: isuni@clarkson.edu

October 31, 2011

To: Roger Westgate, PhD
Center for Autonomous Solar Power (CASP)
Binghamton University
P.O. Box 6000
Binghamton, NY 13902-6000

Re: Progress report, "Electrodeposition of Cu_2ZnSnS_4 (CZTS) with Controlled Stoichiometry"

Executive Summary:

We report the following accomplishment for this project:

- We have begun cyclic voltammetry studies of Cu, Zn, Sn and S in aqueous solutions containing a variety of different complexing agents.

Tasks and Objectives:

Our first objective is to find one or more complexing agents that will shift the equilibrium reduction potentials of Cu and Sn in the cathodic direction. This will allow simultaneous electrodeposition of Cu, Sn and Zn at the same reduction potential. Without complexing agents, the standard reduction potentials of these three elements are:

$$Cu^{2+} + 2e^- \rightarrow Cu \qquad E^0 = +0.340V \; vs. \; NHE$$
$$Zn^{2+} + 2e^- \rightarrow Zn \qquad E^0 = -0.763V \; vs. \; NHE$$
$$Sn^{2+} + 2e^- \rightarrow Sn \qquad E^0 = -0.136V \; vs. \; SHE$$

Without substantially shifting the equilibrium reduction potential for Cu, Cu deposition will be extremely rapid at the highly cathodic potentials at which Zn deposition is possible. In other words, the electrodeposit will contain far more Cu than Zn, so we need to slow Cu electrodeposition through use of a complexing agent. S electrochemistry will also be investigated, but is more complex than that of Cu, Zn and Sn, so the standard reduction potential is not given above.

In addition, we will inspect our cyclic voltammograms for solutions that contain Cu, Zn, Sn and S for evidence of the induced co-deposition mechanism. Evidence for

this would be an anodically shifted equilibrium reduction potential, strong evidence that we might obtain correct stoichiometry for Cu_2ZnSnS_4 at that potential.

Results and Discussion:

A) Citrate

The first complexing agent that we investigated is citrate. The cyclic voltammograms below were obtained on Mo electrodes at a potential scanning rate of 50 mV/sec in solutions that contain 0.5 M Na citrate, 5 mM $CuSO_4$, 5 mM $ZnSO_4$, 5 mM $SnSO_4$ and 20 mM $Na_2S_2O_3$ at pH 4.75. All potentials mentioned are measured against a saturated calomel electrode (SCE) with a Pt counter electrode in a standard three-electrode cell.

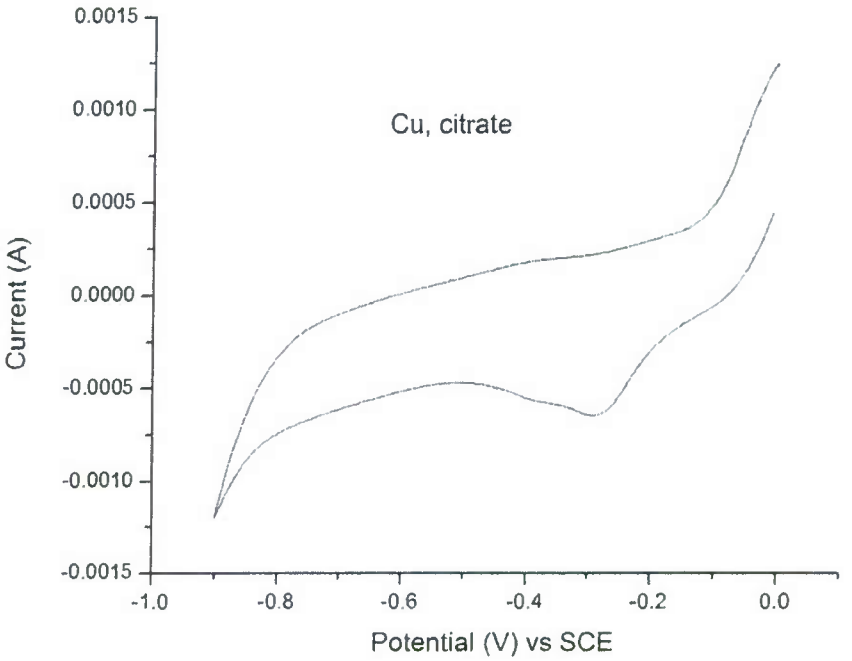

Figure 1. Cyclic voltammogram of 5mM $CuSO_4$ + 0.5 M Na citrate.

Upon addition of citrate, the cathodic peak for Cu was observed at about -0.29 V vs. SCE. This shows that citrate does not form a strong complex with Cu, as there is only a minor shift in the reduction peak when compared to the standard reduction potential of Cu.

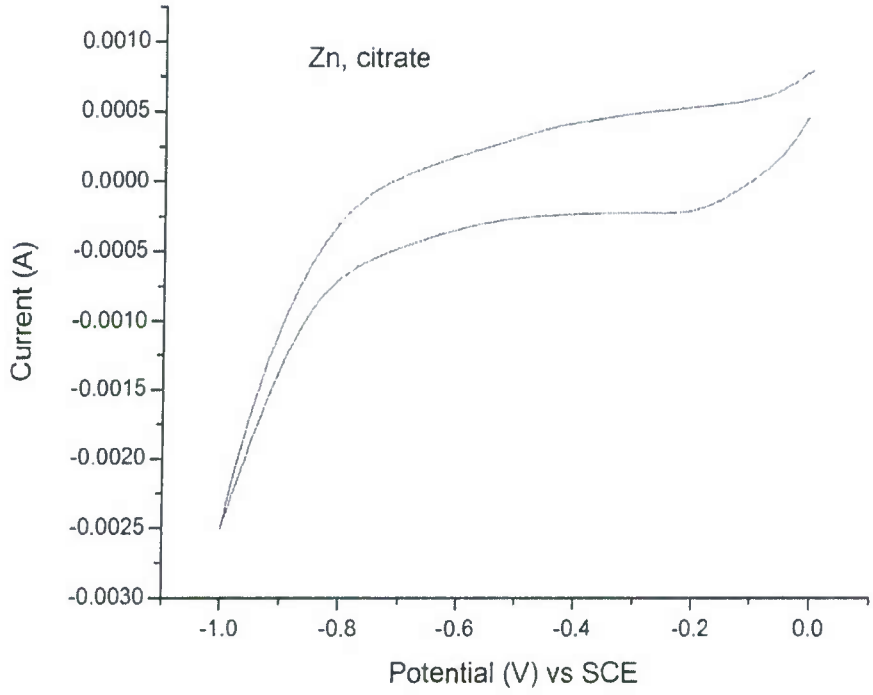

Figure 2. Cyclic voltammogram of 5 mM $ZnSO_4$ + 0.5 M Na citrate.

There was no significant cathodic peak observed for Zn in the potential window of 0.0 to -1.0 V vs. SCE. Therefore in the potential range analyzed, Zn(II) is not reduced.

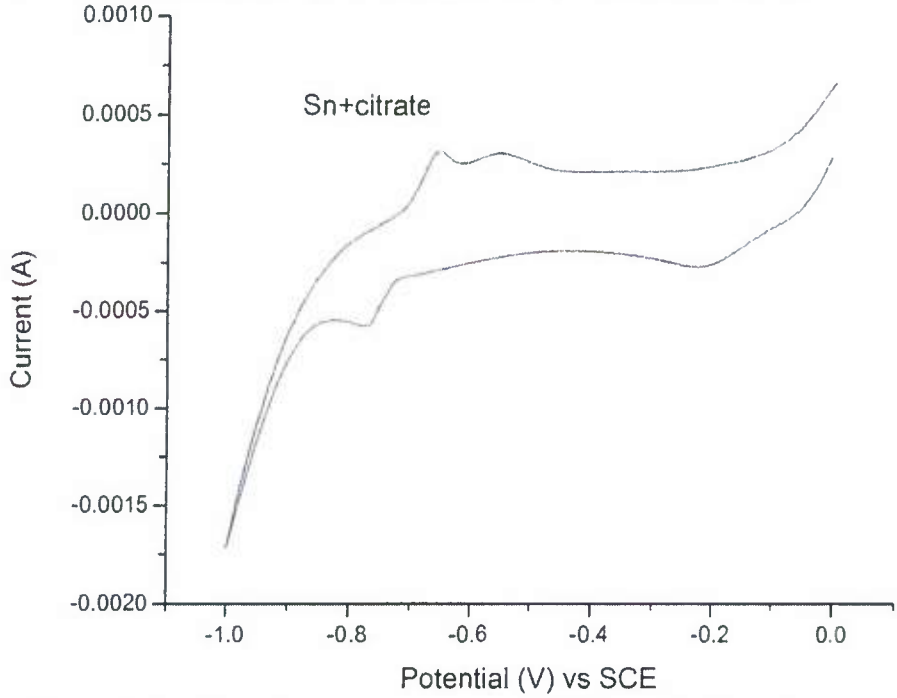

Figure 3. Cyclic voltammogram of 5mM $SnSO_4$ + 0.5 M Na citrate.

Two cathodic peaks were observed at -0.22 V and -0.775 V vs. SCE. A small dip at less cathodic potentials might be related to the reduction of un-complexed Sn(II) and a strong cathodic peak at -0.775 V might be associated with the reduction of complexed Sn (II).

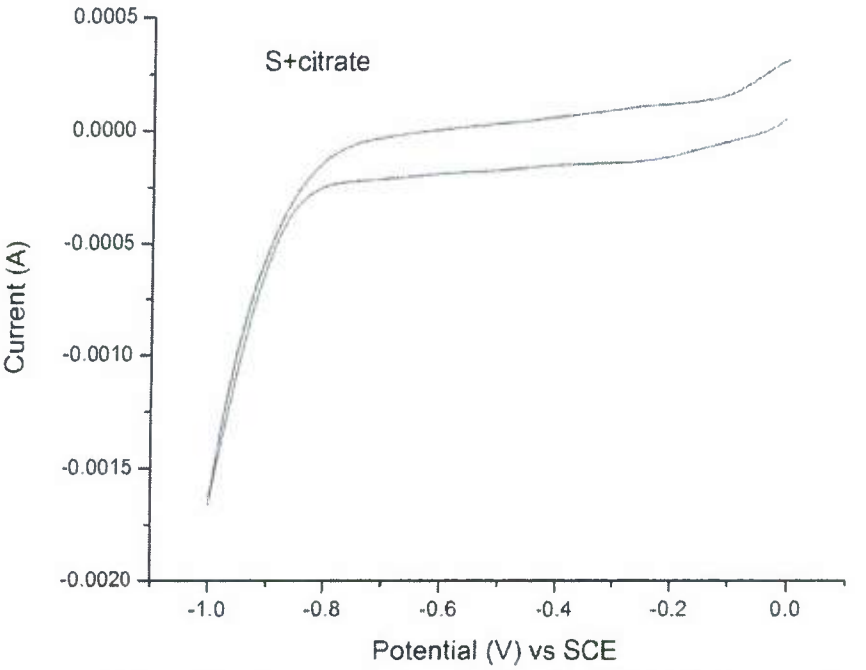

Figure 4. Cyclic voltammogram of 20 mM $Na_2S_2O_3$ + 0.5 M Na citrate.

No reduction peak is observed in the voltammetric studies for S in the presence of citrate.

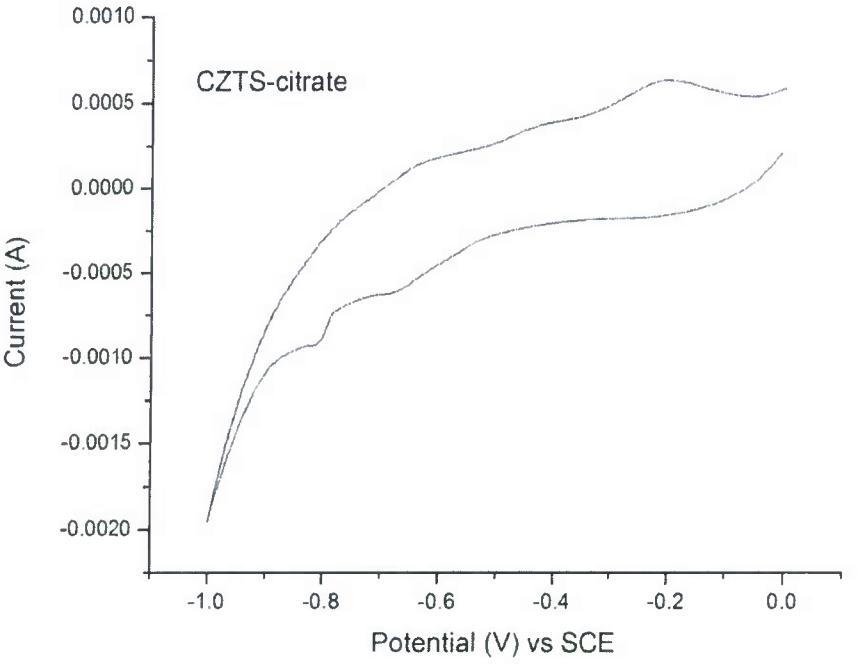

Figure 5. Cyclic voltammogram of 5 mM $CuSO_4$ + 5 mM $ZnSO_4$ + 5 mM $SnSO_4$ + 20 mM $Na_2S_2O_3$ + 0.5 M Na citrate

In the presence of all species (Cu, Zn, Sn, S) in the same bath, we observed two cathodic peaks at -0.685 V and -0.81 V. We observed no anodically shifted cathodic peaks, so we see no evidence for the induced co-deposition mechanism.

B) Glucuronic acid

The effect of glucuronic acid ($C_6H_{10}O_7$) as a complexing agent was also studied. This choice was based upon literature reports of gluconate as a complexing agent for Cu and Zn electrodeposition. All the experiments with glucuronic acid as the complexing agent were carried out at pH 2.75.

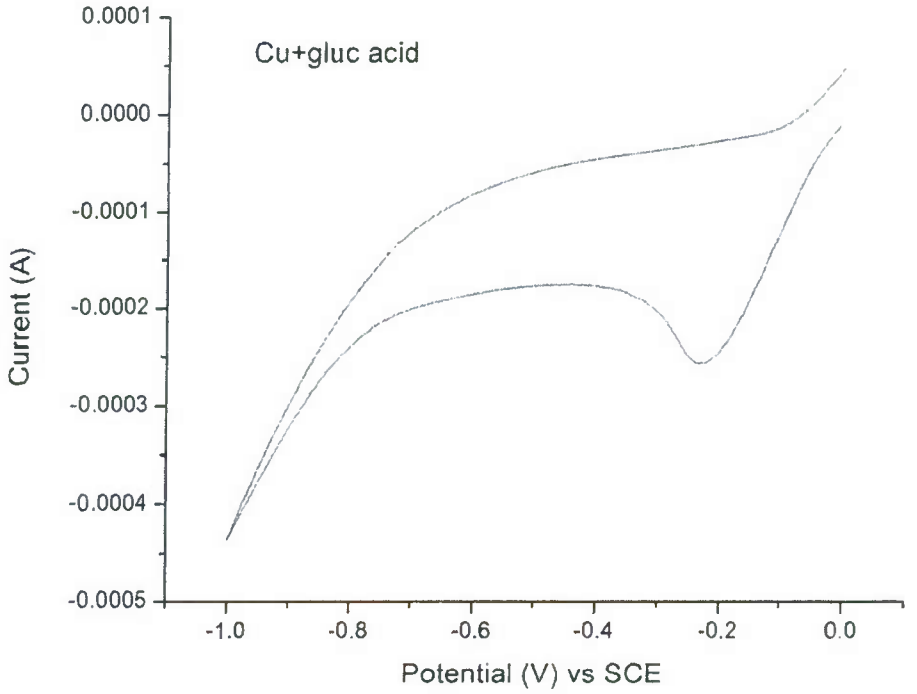

Figure 6. Cyclic voltammogram of 5mM $CuSO_4$ + 25 mM glucuronic acid.

The behavior of Cu in the presence of glucuronic acid resembles to that of Cu in the presence of citrate. Cu does not form a strong complex with glucuronic acid and hence the reduction peak is observed only at -0.235 V vs. SCE, only modestly shifted from its value for uncomplexed Cu(II).

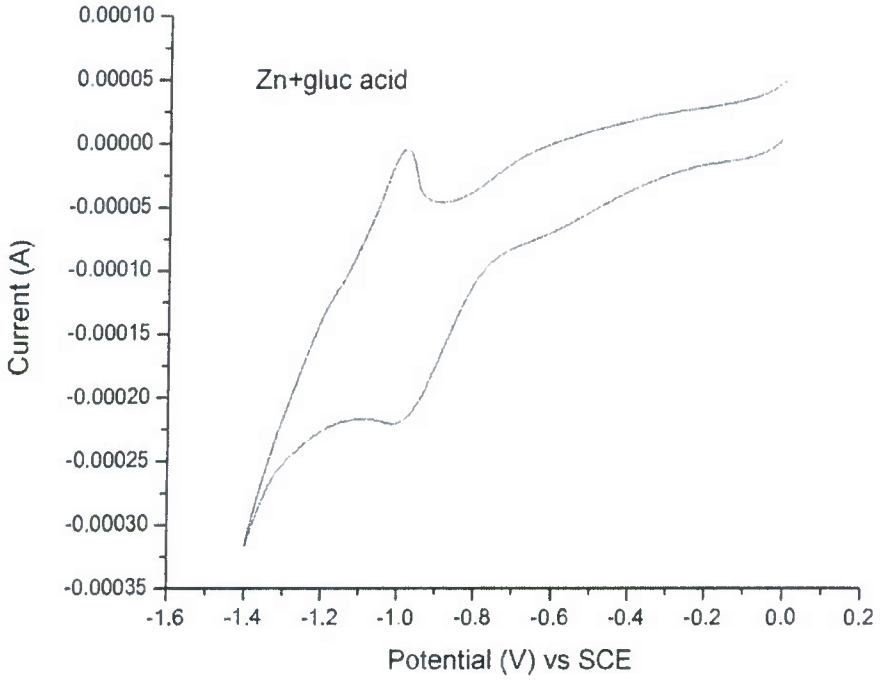

Figure 7. Cyclic voltammogram of 5mM $ZnSO_4$ + 25 mM glucuronic acid.

A strong cathodic peak was observed at -1.0 V for Zn. But, the reduction potentials of Cu and Zn are still far apart in the presence of glucuronic acid.

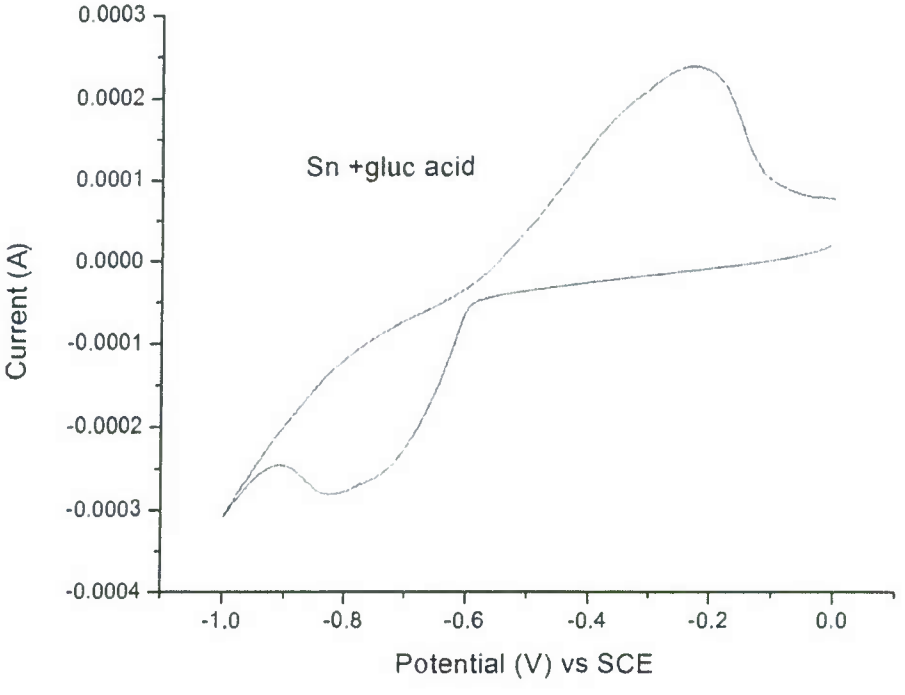

Figure 8. Cyclic voltammogram of 5 mM $SnSO_4$ + 25 mM glucuronic acid.

A broad cathodic peak was observed around -0.83 V in the presence of Sn and glucuronic acid, suggesting strong complex formation.

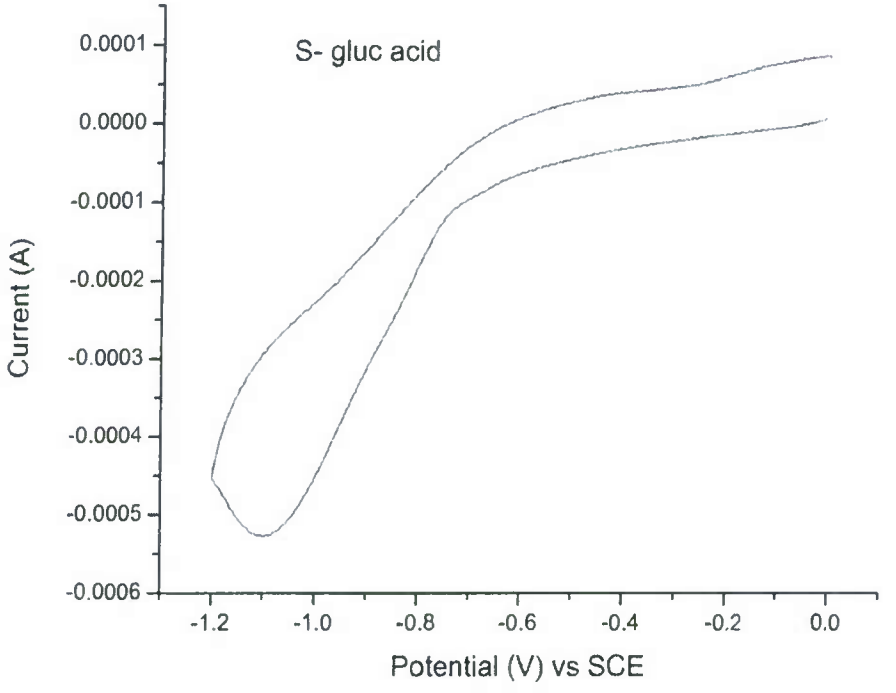

Figure 9. Cyclic voltammogram of 20 mM $Na_2S_2O_3$ + 25 mM glucuronic acid.

A broad cathodic peak was observed at -1.1 V for S in the presence of glucuronic acid.

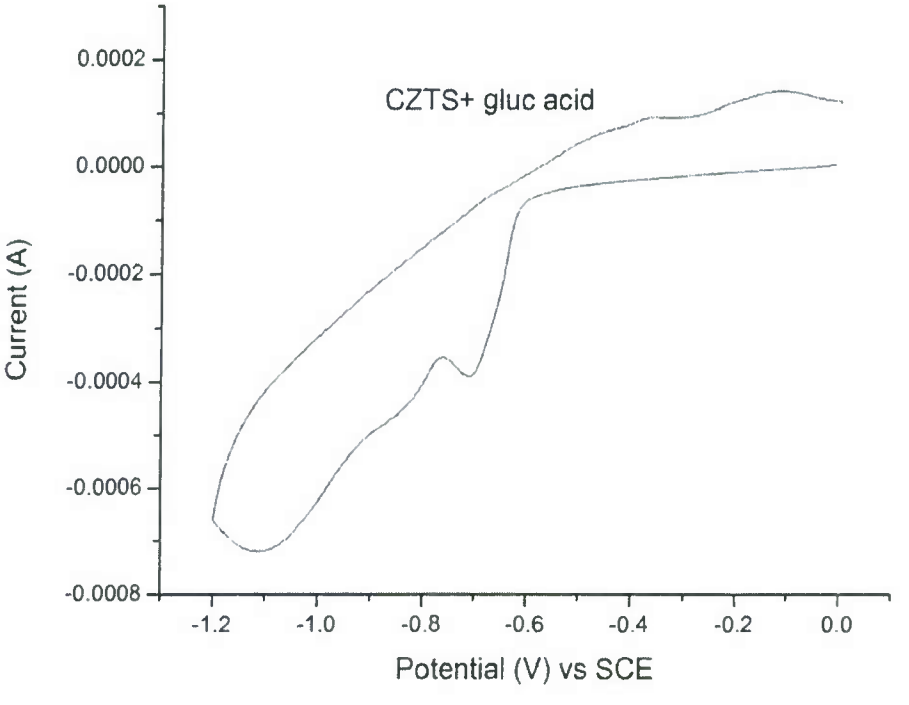

Figure 10. Cyclic voltammogram of 5 mM $CuSO_4$ + 5 mM $ZnSO_4$ + 5 mM $SnSO_4$ + 20 mM $Na_2S_2O_3$ + 25 mM glucuronic acid.

Two cathodic peaks were observed at -0.71 V (sharp) and -1.1 V (broad). Again, no anodically shifted cathodic peaks are observed, so we see no evidence for the induced co-deposition mechanism.

C) Glycine

The literature suggests that amines are good complexing agents for Zn and Sn, so glycine was also studied. All the experiments were carried out at a pH of 4.5.

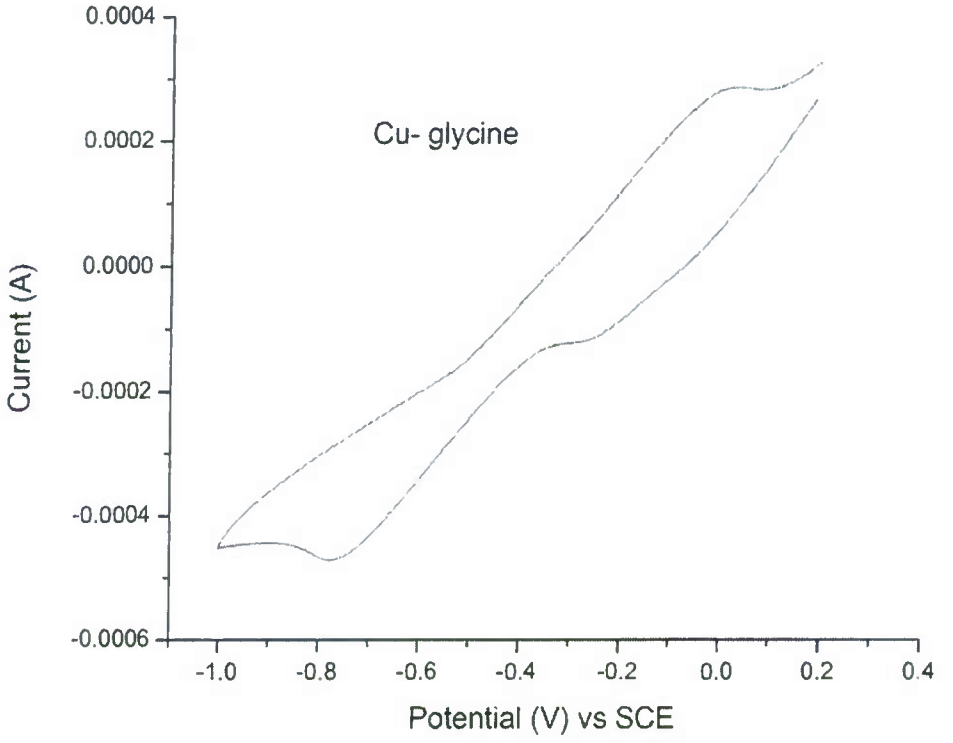

Figure 11. Cyclic voltammogram of 5 mM $CuSO_4$ + 0.25 M glycine.

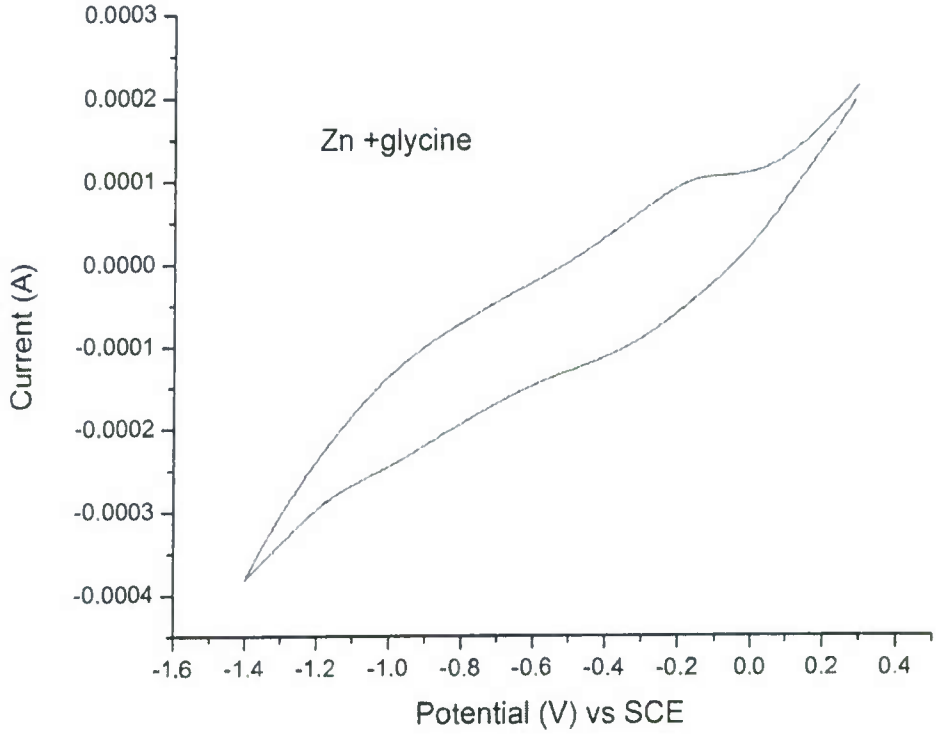

Figure 12. Cyclic voltammogram of 5 mM $ZnSO_4$ + 0.25 M glycine.

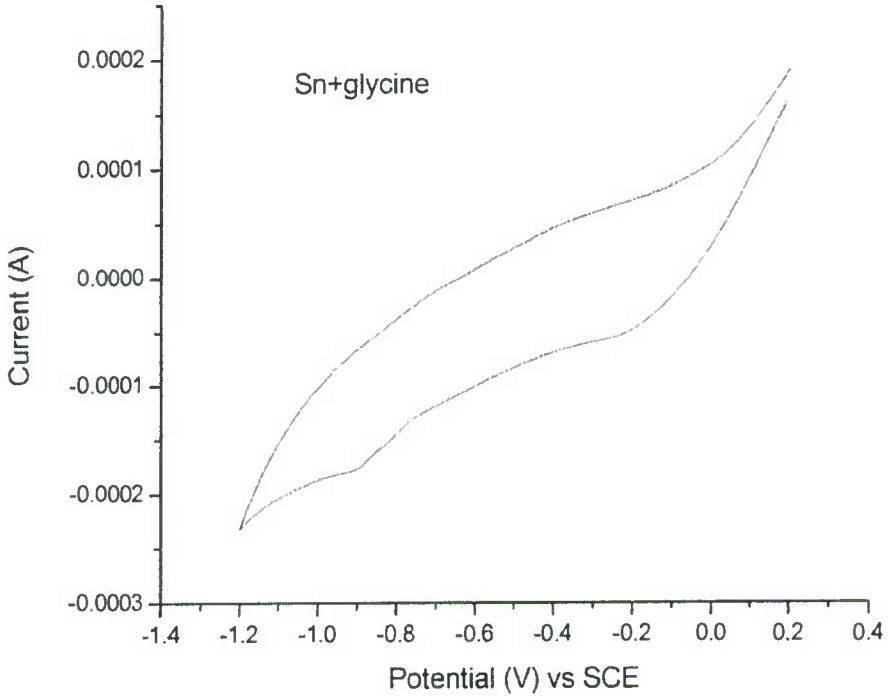

Figure 13. Cyclic voltammogram of 5 mM $SnSO_4$ + 0.25 M glycine.

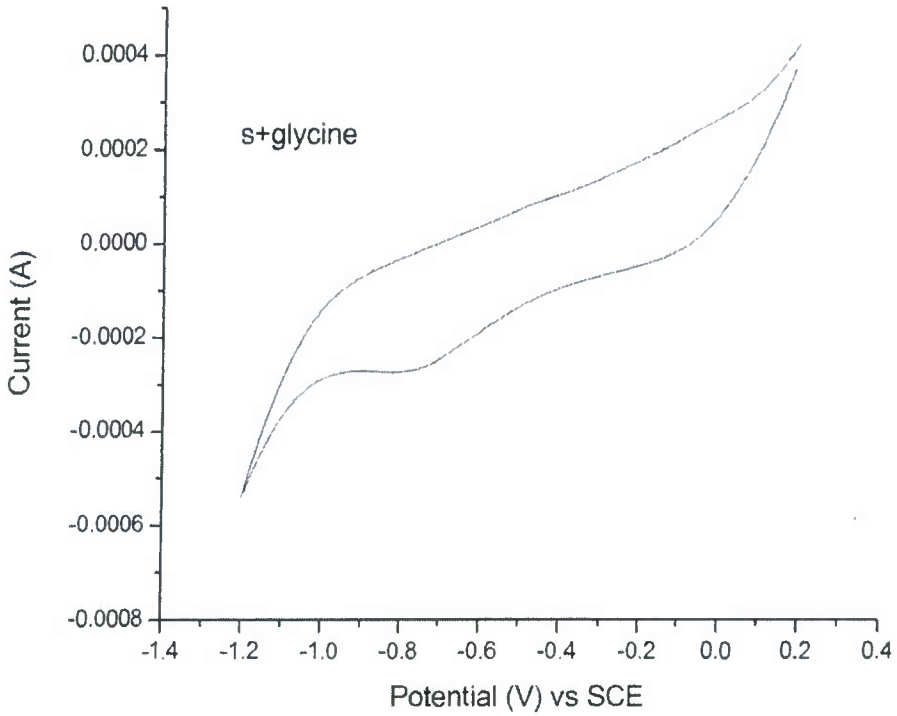

Figure 14. Cyclic voltammogram of 20 mM $Na_2S_2O_3$ + 0.25 M glycine.

From the above cyclic voltammograms, we see a similar trend in the presence of Cu(II), Zn(II), Sn(II) and S, very broad and indistinct cathodic features.

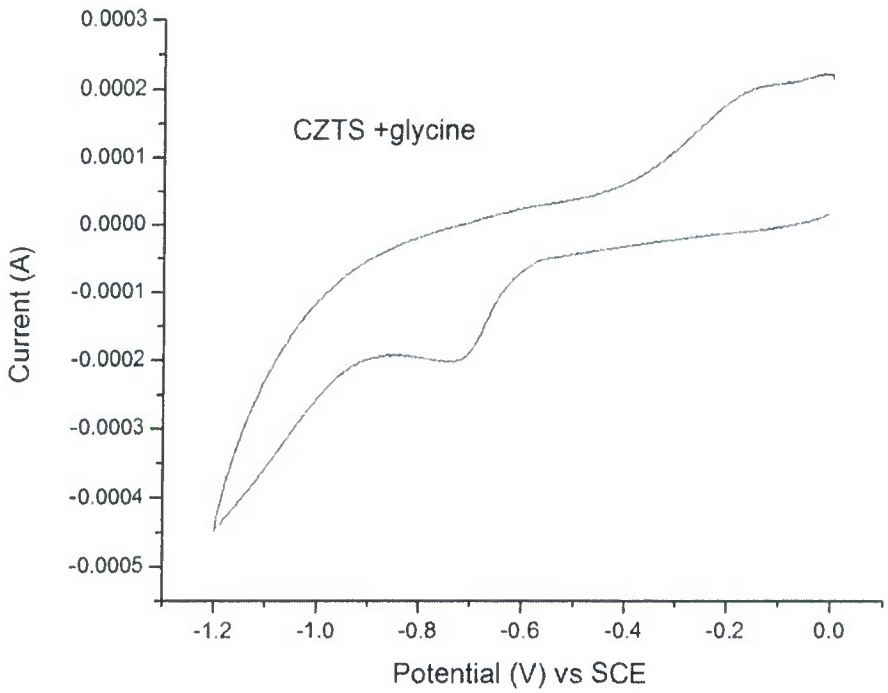

Fig 15. Cyclic voltammogram of 5 mM $CuSO_4$ + 5 mM $ZnSO_4$ + 5 mM $SnSO_4$ + 20 mM $Na_2S_2O_3$ + 0.25 M glycine.

The cyclic voltammogram with all the elements in the same bath exhibits a cathodic peak at -0.725 V, which does not correspond to the one step reduction of CZTS.

D) Thiocyanate (SCN^-)

From, the previous research, we know that Cu(II) forms strong complexes with thiocyanate, so this was also studied. All the experiments with thiocyanate as the complexing agent were performed at a pH of 1.75.

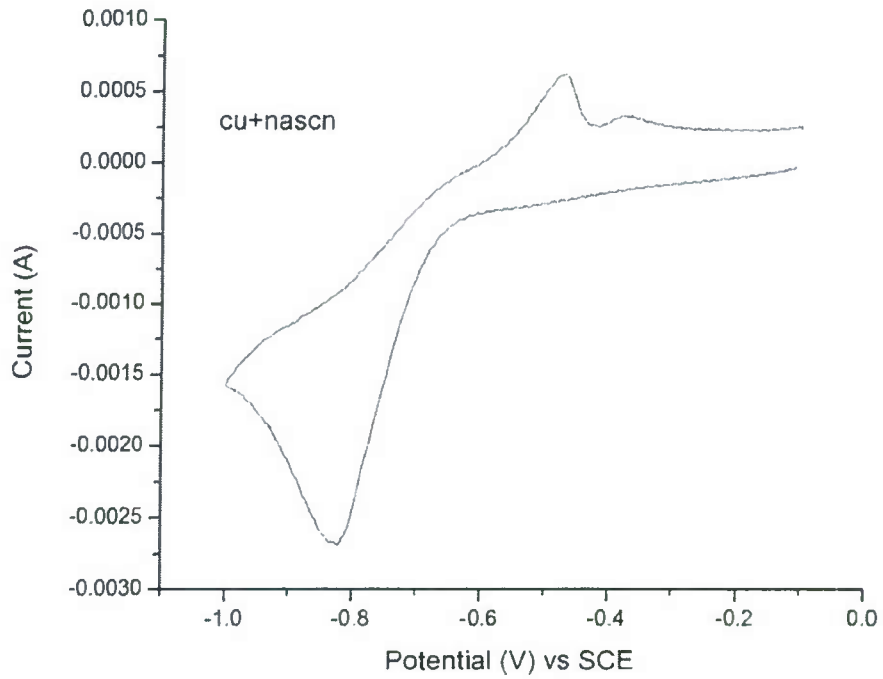

Figure 16. Cyclic voltammogram of 5 mM $CuSO_4$ + 2 M NaSCN.

The cyclic voltammogram of Cu in the presence of thiocyanate shows a strong cathodic peak at -0.825 V, showing that thiocyanate forms a strong Cu(II) complex, dramatically shifting the reduction potential of Cu(II) in the cathodic direction. This is the largest effect of any complexing agent studied so far.

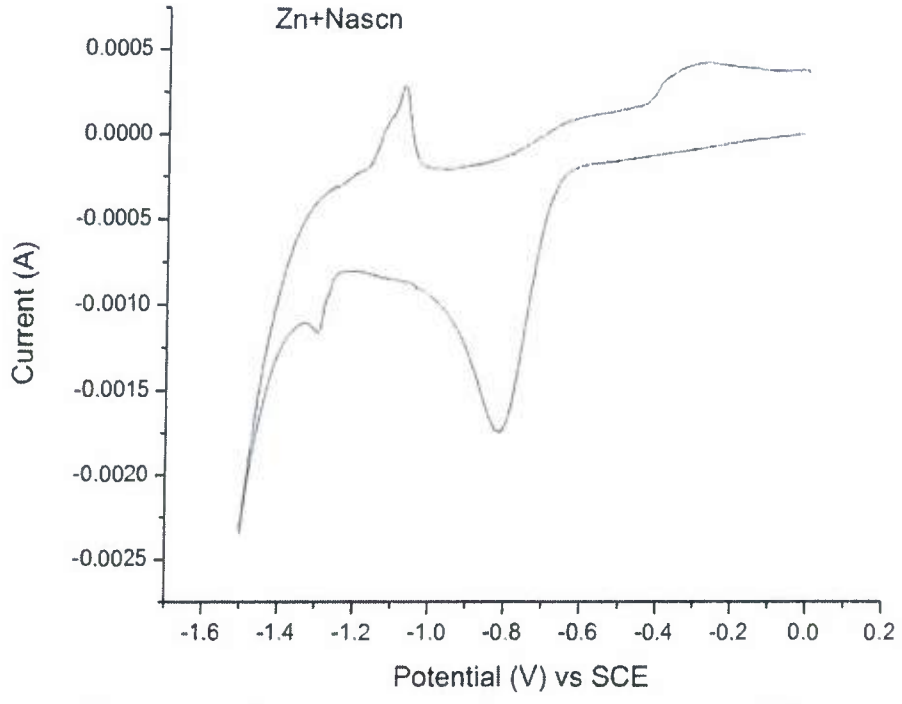

Figure 17. Cyclic voltammogram of 5 mM $ZnSO_4$ + 2 M NaSCN.

The cyclic voltammogram of Zn in the presence of thiocyanate shows two cathodic peaks at -0.815V and -1.3 V. The cathodic peak at -0.815 V is close to the reduction peak observed in complexed Cu, which is promising.

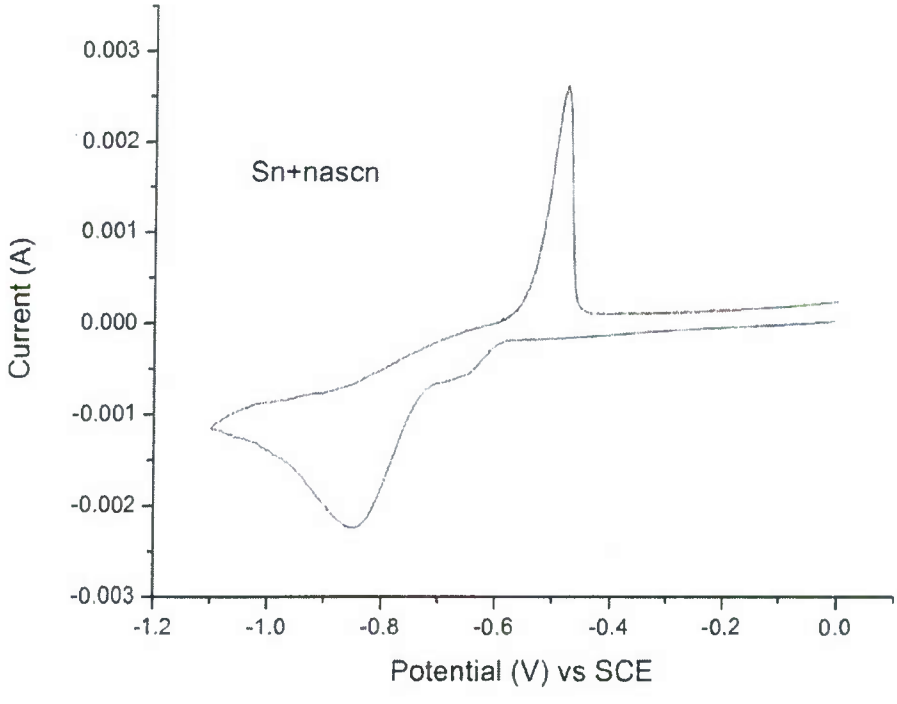

Figure 18. Cyclic voltammogram of 5 mM $SnSO_4$ + 2 M NaSCN.

There are two reduction peaks observed at -0.65 V and -0.85 V in the solution of Sn(II) and thiocyanate, showing some complex formation.

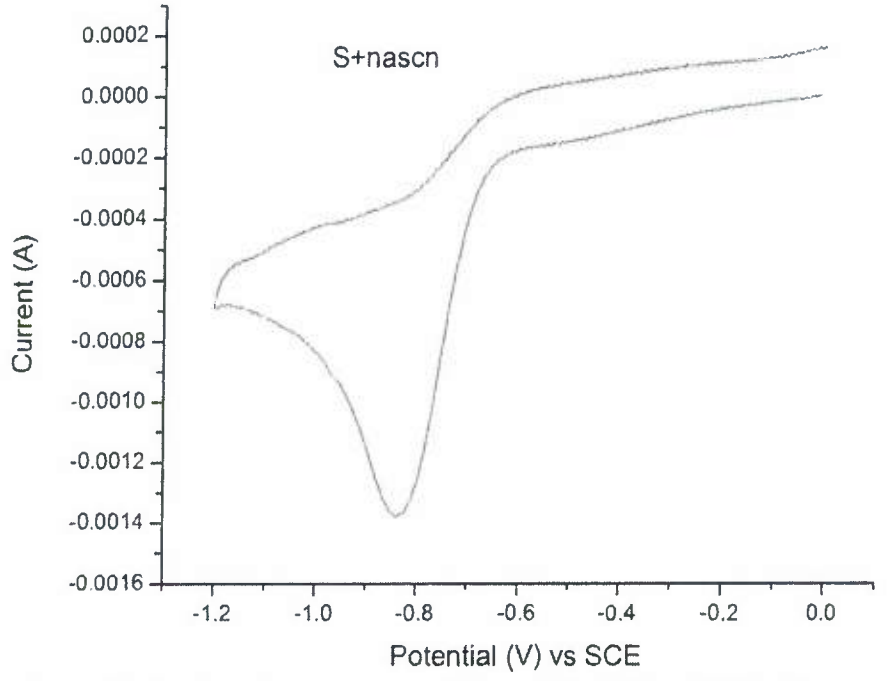

Figure 19. Cyclic voltammogram of 20 mM $Na_2S_2O_3$ + 2 M NaSCN.

Coincidently, a strong cathodic peak was observed at -0.84 V for sulphur in the presence of thiocyanate.

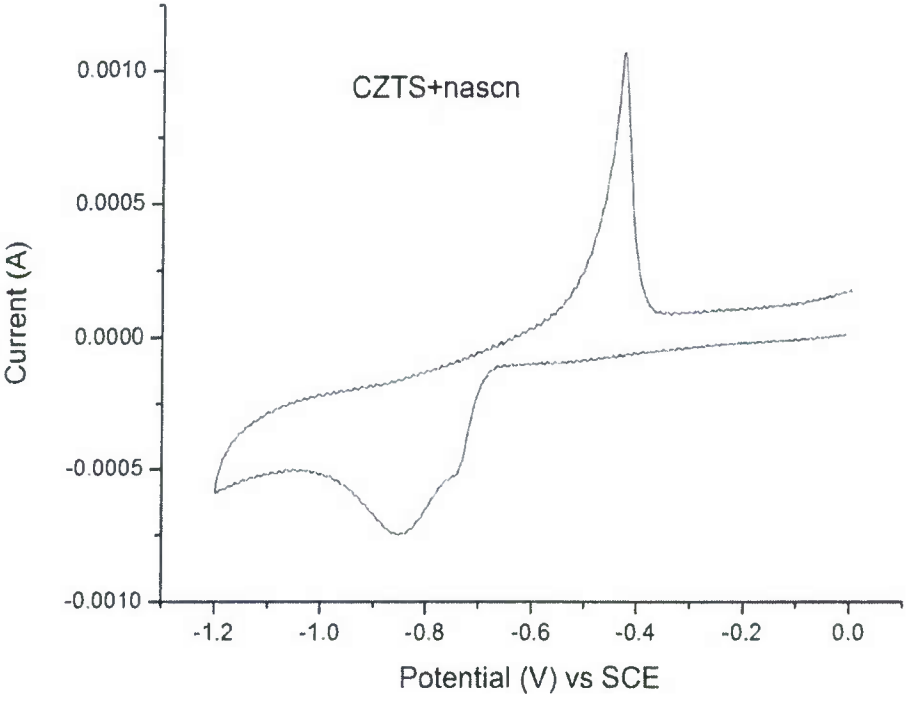

Figure 20. Cyclic voltammogram of 5 mM $CuSO_4$ + 5 mM $ZnSO_4$ + 5 mM $SnSO_4$ + 20 mM $Na_2S_2O_3$ + 2 M NaSCN.

Though we did not observe an anodically shifted cathodic peak in the case of thiocyanate as the complexing agent, we observed two (non-shifted) different peaks at -0.75 V and -0.85 V. Thiocyanate does seem to be promising, since the reduction potentials of all the individual elements were fairly close to each other (within ~ 50 mV).

E) Tartaric acid

The combined effect of citrate and tartarate has been previously studied, so we analyzed the effect of tartaric acid as a comlexing agent. All the experiments with tartaric acid ($C_4H_6O_6$) were performed at a pH of 4.75.

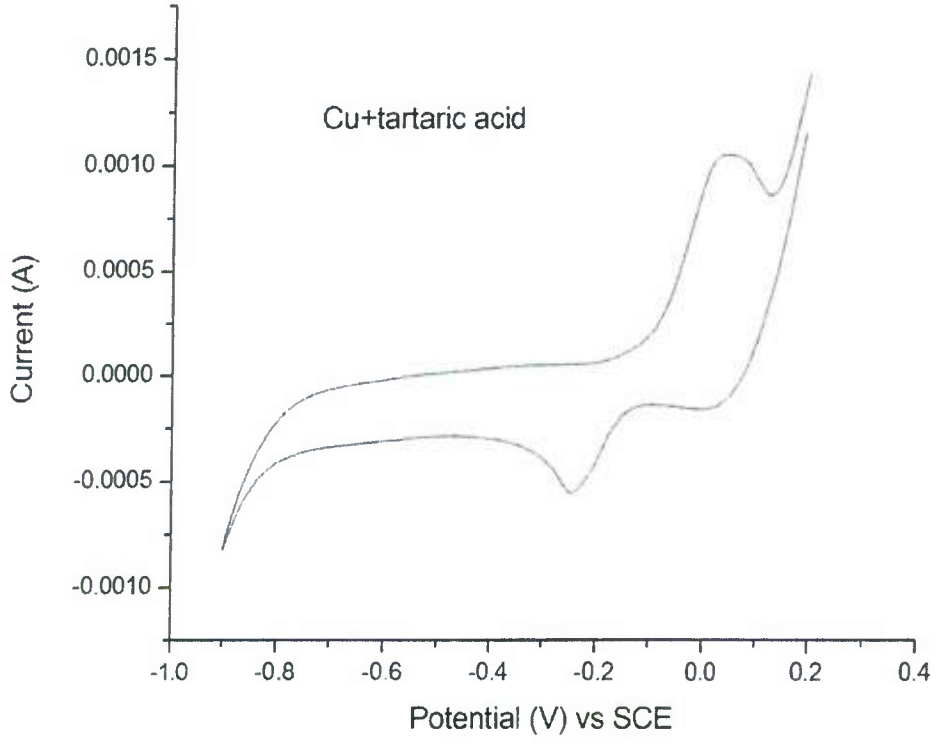

Figure 21. Cyclic voltammogram of 5 mM $CuSO_4$ + 0.25 M tartaric acid.

From this figure, it can be clearly seen that tartaric acid does not cathodically shift the reduction potential of Cu(II).

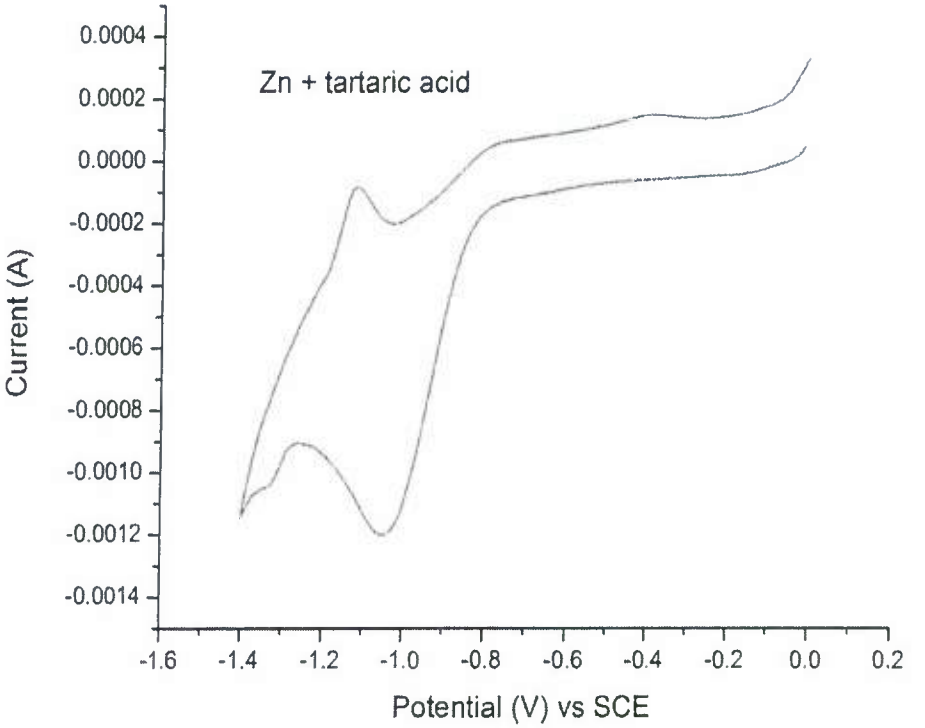

Figure 22. Cyclic voltammogram of 5 mM $ZnSO_4$ + 0.25 M tartaric acid.

A cathodic peak is observed at -1.05 V in the case of Zn(II) which is more cathodic to the reduction potential observed in the case of Cu(II).

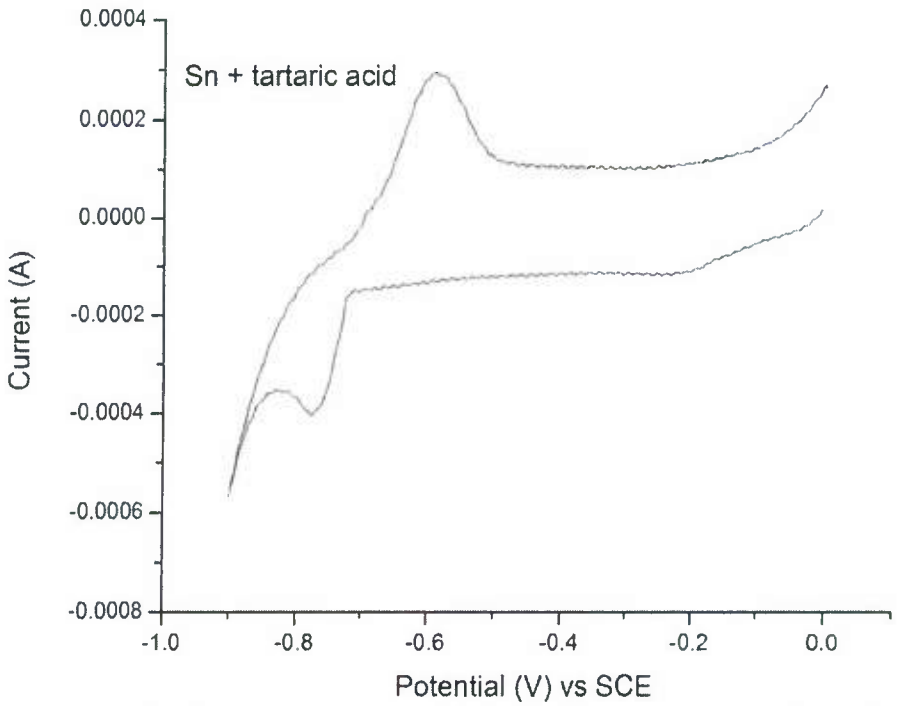

Figure 23. Cyclic voltammogram of 5 mM $SnSO_4$ + 0.25 M tartaric acid.

A cathodic peak was observed in the case of Sn(II) with tartaric acid at -0. 78 V, suggesting strong complex formation.

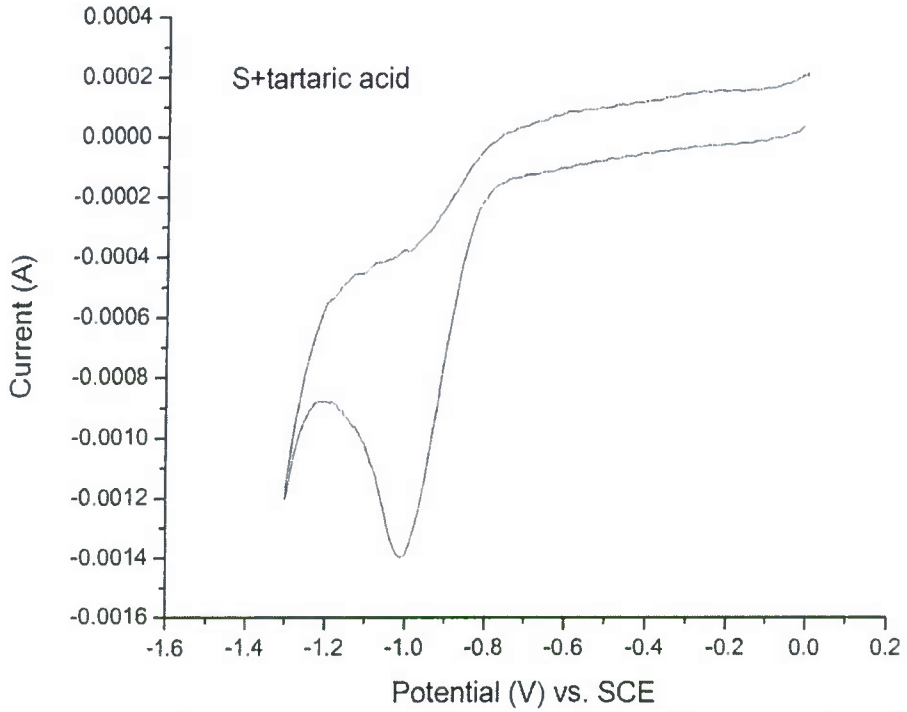

Figure 24. Cyclic voltammogram of 20 mM $Na_2S_2O_3$ + 0.25 M tartaric acid.

The cathodic peak observed for S is close to that for Zn(II), which is about -1.0 V.

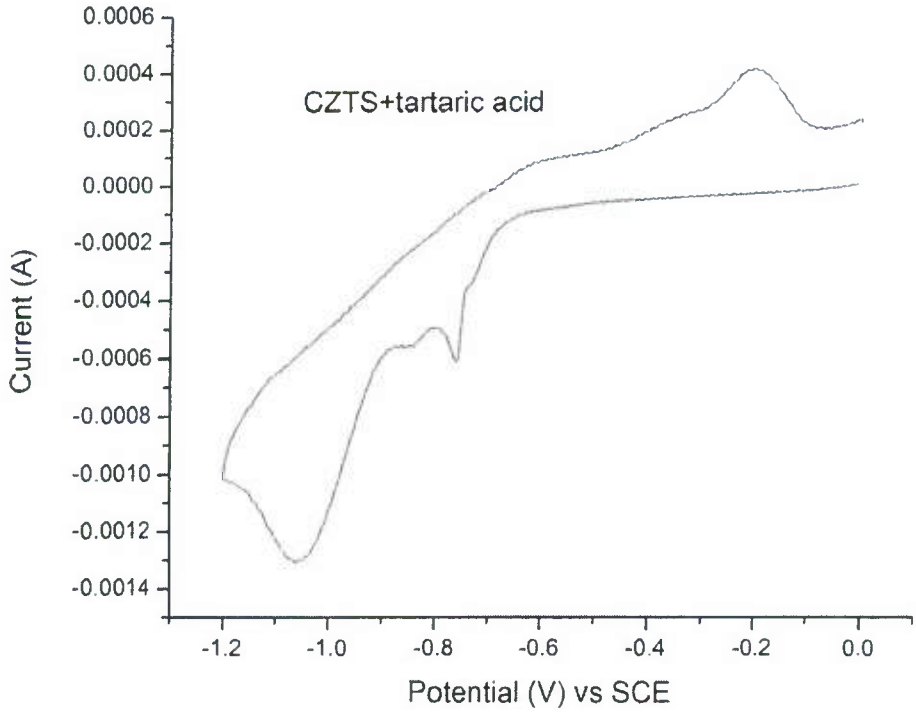

Figure 25. Cyclic voltammogram of 5 mM $CuSO_4$ + 5 mM $ZnSO_4$ + 5 mM $SnSO_4$ + 20 mM $Na_2S_2O_3$ + 0.25 M tartaric acid.

The bath that contains all the precursors for CZTS showed three cathodic peaks at -0.763 V, -0.85 V and -1.05 V. However, none of them corresponds to an anodically shifted peak where induced co-deposition might take occur.

All of the results from above are tabulated in the following table.

Table 1. Potentials at which reduction of individual elements is observed in the presence of different complexing agents.

Complexing agent	pH	Cu(II)	Zn(II)	Sn(II)	S(VI)	CZTS
Citrate	4.75	E_1=-0.29V	*	E_1=-0.22V E_2= -0.775V	*	E_1= -0.685V E_2=-0.81V
Glucuronic acid	2.75	E_1=-0.235V	E_1=-1.0V	E_1=-0.835V	E_1=-1.1V	E_1= -0.71V E_2=-1.1V
Glycine	4.5	E_1=-0.775V	*	E_1=-0.9V	E_1=-0.775V	E_1=-0.725V
NaSCN	1.75	E_1=-0.825V	E_1=-0.815V E_2= -1.3V	E_1=-0.65V E_2= -0.85V	E_1=-0.84V	E_1=-0.85V A hump at -0.75V
Tartaric acid-0.25M	4.75	E_1=-0.25V	E_1=-1.05V	E_1=-0.778V	E_1=-1.0V	E_1=-0.763V E_2= -0.85V E_3=-1.05V

Future Plans:

- We plan to continue measuring cyclic voltammograms of Cu, Zn and Sn in different aqueous solutions to find one or more complexing agents that shift the equilibrium reduction potential of both Cu and Sn in the cathodic direction. **So far, thiocyanate (SCN^-) appears to be the most promising complexing agent.**
- Combinations of more than one complexing agent will also be investigated.
- We will obtain cyclic voltammograms for solutions that contain Cu, Zn, Sn and S and inspect them for evidence of the induced co-deposition mechanism. Evidence for this would be an anodically shifted equilibrium reduction potential.

- Should we observe such an anodically shifted reduction potential, then we will investigate the stoichiometry of electrodeposition at that potential using energy dispersive x-ray spectroscopy (EDX).
- We will also being to study the composition of electrodeposits (using EDX) even when an anodically shifted reduction peak is not observed.

Overall Project Status:

- We are beginning to investigate the different complexing agents that might be needed for electrodeposition of Cu_2ZnSnS_4 (CZTS) with controlled stoichiometry.

Sincerely,

Ian Suni